

**AN APPROACH TO DYNAMICS AND CONTROL OF FLEXIBLE  
SPACE STRUCTURE**

By

**YUAN CHEN**

B. A. Sc. (Electrical Engineering), Shanghai Jiao Tong University, 1982

**A THESIS SUBMITTED IN PARTIAL FULFILLMENT OF  
THE REQUIREMENTS FOR THE DEGREE OF  
MASTER OF APPLIED SCIENCE**

in

**THE FACULTY OF GRADUATE STUDIES  
MECHANICAL ENGINEERING**

We accept this thesis as conforming  
to the required standard

**THE UNIVERSITY OF BRITISH COLUMBIA**

April 1993

© YUAN CHEN, 1993

In presenting this thesis in partial fulfilment of the requirements for an advanced degree at the University of British Columbia, I agree that the Library shall make it freely available for reference and study. I further agree that permission for extensive copying of this thesis for scholarly purposes may be granted by the head of my department or by his or her representatives. It is understood that copying or publication of this thesis for financial gain shall not be allowed without my written permission.

(Signature)

Department of Mechanical Engineering

The University of British Columbia  
Vancouver, Canada

Date 29/04/93

## Abstract

A relatively general formulation for studying dynamics and control of a large class of systems, characterized by interconnected rigid bodies, beam and plate type structural members forming a tree topology with two level of branching, is developed using the Lagrangian procedure. The governing equations are discretized using two fundamentally different approaches of system and component modes synthesis. Versatility of the formulation is demonstrated, through its application to two systems of contemporary interest, in the presence of nonlinear control: (i) Space station based, two-arm mobile, flexible manipulator; (ii) NASA proposed configuration involving a flexible slewing arm abode a flexible truss with a rigid antenna. Relative merit of the two discretization procedures is assessed over a range of system parameters through comparison of the controlled and uncontrolled responses. Results suggest that the component mode synthesis, though relatively easy to implement, can lead to inaccurate response unless the boundary conditions are modeled precisely. Unfortunately, this is seldom possible, particularly with complex systems of current interest. On the other hand, discretization through system modes, though precise, would require frequent updating leading to an increase in the computational time. The investigation represents an original contribution of far-reaching consequence to the field. Such a planned approach to assess discretization methodologies with reference to space based system has not be reported in open literature.

## Table of Contents

<b>Abstract</b>	<b>ii</b>
<b>List of Figures</b>	<b>v</b>
<b>List of Tables</b>	<b>viii</b>
<b>List of Symbols</b>	<b>ix</b>
<b>Acknowledgement</b>	<b>xiii</b>
<b>1 INTRODUCTION</b>	<b>1</b>
1.1 Preliminary Remarks . . . . .	1
1.2 Background to the Problem . . . . .	2
1.3 Scope of the Present Investigation . . . . .	6
<b>2 KINEMATICS OF THE SYSTEM</b>	<b>8</b>
2.1 Coordinate System . . . . .	10
2.2 Position of Spacecraft in Space . . . . .	13
2.3 Shift in the Center of Mass . . . . .	16
2.4 Elastic and Thermal Deformations . . . . .	17
2.4.1 Background . . . . .	17
2.4.2 Deformation Expression for Beam-type Substructure . . . . .	19
2.4.3 Thermal Deformation . . . . .	20
2.4.4 Transverse vibration . . . . .	21

2.5	Rotation Matrices . . . . .	22
<b>3</b>	<b>KINETICS OF THE SYSTEM</b>	<b>24</b>
3.1	Kinetic Energy . . . . .	24
3.2	Potential Energy . . . . .	26
3.3	Equations of Motion . . . . .	27
<b>4</b>	<b>AN APPROACH TO CONTROL</b>	<b>31</b>
4.1	Feedback Linearization Technique (FLT) . . . . .	31
4.2	Control Implementation Procedures . . . . .	35
<b>5</b>	<b>COMPUTATIONAL CONSIDERATIONS</b>	<b>38</b>
5.1	Program Structure of the Component Modes Method (CMM) . . . . .	38
5.2	Program Structure for the System Modes Method (SMM) . . . . .	40
<b>6</b>	<b>RESULTS AND DISCUSSION</b>	<b>45</b>
6.1	Two Link Mobile Servicing System . . . . .	45
6.2	NASA's Control-Structure Interaction Model . . . . .	59
<b>7</b>	<b>CONCLUDING REMARKS AND RECOMMENDATIONS FOR FUTURE WORK</b>	<b>64</b>
	<b>Bibliography</b>	<b>66</b>
<b>A</b>	<b>DETAILS OF <math>T_{sys}</math>, <math>I_{sys}</math> AND <math>\bar{H}_{sys}</math></b>	<b>70</b>
<b>B</b>	<b>INPUT FILES FOR THE CMM</b>	<b>79</b>
<b>C</b>	<b>INPUT DATA FILES FOR THE SMM</b>	<b>81</b>

## List of Figures

1.1	One of the earlier configurations of the proposed space station <i>Freedom</i> . . . . .	3
1.2	Schematic diagrams of the four milestone Configurations of the evolving space station <i>Freedom</i> : (a) First Milestone Configuration (FMC) (b) Man Tended Configuration (MTC) (c) Permanently Manned Configuration (PMC) (d) Assembly Complete Configuration (ACC). . . . .	4
2.3	A system of interconnected bodies, forming two levels of branching, considered for study. It can represent a vast variety of systems including the proposed space station. . . . .	9
2.4	Body fixed coordinate system $F_p(X_p, Y_p, Z_p)$ and the solar radiation incident angles. . . . .	11
2.5	Coordinate systems used to identify position of a mass element undergoing rigid body as well as vibrational motions and thermal deformations. . . . .	12
2.6	Orbital parameters for a spacecraft defining position of its center of mass. . . . .	14
2.7	Modified Eulerian rotations specifying arbitrary orientation of the system in space. . . . .	15
4.8	Block diagram of a feedback linearized control system . . . . .	34
4.9	Block diagram of the Quasi-closed loop control system . . . . .	37
5.10	Program flow-chart for the CMM simulation . . . . .	39
5.11	Flow-chart showing the numerical integration procedure using the CMM . . . . .	41
5.12	Program flow-chart for the system modes determination. . . . .	42

5.13	Program flow-chart for the SMM simulation . . . . .	43
6.14	Geometry of the two-link manipulator supported by a rigid space platform.	47
6.15	Effect of increasing the amplitude as well as speed of the slewing maneuver, in the plane of the orbit, with the MSS located at the center of the station: (a) 45° in 10 min; (b) 90° in 10 min; (c) 180° in 10 min. . . . .	50
6.16	Effect of the slewing speed on the system response with the manipulator at the center of the main truss. The slewing maneuver of 180°(inplane) is completed in: (a) 10 min; (b) 5 min; (c) 2 min. . . . .	51
6.17	Response plots showing the effect of the manipulator's location: (a) Ma- nipulator at the center of the station; (b) manipulator at the tip of the station. The slewing rate is 180° in 10 min. . . . .	52
6.18	Response plots showing the effect of the manipulator's location during the slewing maneuver of 180° in 5 min. (a) manipulator at the center of the station (b) manipulator at the tip of the station. . . . .	53
6.19	Controlled response using the FLT applied to the librational degrees of freedom with the manipulator at the center of the station: slewing ma- neuver of 45° in 10 minutes. . . . .	54
6.20	Controlled response using the FLT applied to the librational degrees of freedom with the manipulator at the center of the station: slewing ma- neuver of 90° in 10 minutes. . . . .	55
6.21	Controlled response using the FLT applied to the librational degrees of freedom with the manipulator at the center of the station: slewing ma- neuver of 180° in 10 minutes. . . . .	56
6.22	System response in the presence of FLT control with the manipulator located at the tip of the station: slewing maneuver of 180° in 10 minutes.	57

6.23	System response in the presence of FLT control with the manipulator located at the tip of the station: slewing maneuver of $180^\circ$ in 5 minutes.	58
6.24	Geometry of the model proposed by NASA for the Control-Structure-Interaction (CSI) study. . . . .	61
6.25	Response of the NASA's CSI model during a $180^\circ$ maneuver in 10 minutes: (a) discretization using the CMM; (b) discretization using the SMM. The manipulator is located at the center of the truss. . . . .	62
6.26	Effect of the manipulator location on the system response during the $180^\circ$ slewing maneuver in 10 minutes: (a) discretization using the CMM; (b) discretization using the SMM. The manipulator is situated at the tip of the truss. . . . .	63

## List of Tables

6.1	Numerical values used in simulation of the two-link manipulator . . . . .	46
6.2	Numerical values used during simulation of the CSI configuration dynamics	60

## List of Symbols

$a_b$	beam radius
$\bar{d}_i, \bar{d}_{i,j}$	position vectors from $O_c$ to $O_i$ and $O_i$ to $O_{i,j}$ , respectively
$dm_c, dm_i, dm_{i,j}$	elemental mass in body $B_c, B_i$ , and $B_{i,j}$ , respectively
$i$	orbit inclination with respect to the ecliptic plane
$k_b$	thermal conductivity of an appendage
$\bar{l}$	direction cosines of $\bar{R}_{cm}$ with respect to $X_p, Y_p, Z_p$ axes
$l_b$	beam length
$l_b^*$	thermal reference length of the beam
$l_c, l_i, l_{i,j}$	length of bodies $B_c, B_i$ and $B_{i,j}$ , respectively
$m_b$	beam mass per unit length
$m_c, m_i, m_{i,j}$	mass of bodies $B_c, B_i$ and $B_{i,j}$ , respectively
$n_i$	number of $B_{i,j}$ bodies attached to body $B_i$
$\bar{q}_f, \bar{q}_r$	vector representing flexible and rigid generalized coordinates
$(\bar{q}_r)_d$	vector representing the desired value of the rigid generalized coordinates
$q_s$	solar radiation intensity; $W/m^2$
$t$	time
$v^b, w^b$	transverse vibration of a beam in its Y and Z directions, respectively
$C_i^c, C_{i,j}^c$	transformation matrices defining orientation of $F_i, F_{i,j}$ relative to $F_c$ , respectively

$\bar{C}_{cm}$	$\bar{C}_{cm}^f + \bar{C}_{cm}^i$
$\bar{C}_{cm}^f$	position vector from $C^i$ to the instantaneous center of mass of the spacecraft
$\bar{C}_{cm}^i$	position vector from $O_c$ to the center of mass of the undeformed spacecraft
$C^i, C^f$	center of mass of the undeformed and deformed configurations of the spacecraft, respectively
$EI_{yy}, EI_{zz}$	flexural rigidity of a beam about its Y and Z axes, respectively
$\bar{H}_{sys}$	angular momentum of the spacecraft with respect to the $X_c, Y_c, Z_c$ axes, respectively
$I_{sys}$	inertia matrix of spacecraft with respect to the $X_c, Y_c, Z_c$ axes, respectively
$I_{xx}, I_{yy}, I_{zz}$	principal inertia of body $B_k$ about $X_k, Y_k, Z_k$ axes, respectively; $k = c, i$ or $i, j$
$M$	total mass of spacecraft
$N, N_j$	total number of $B_i$ and $B_{i,j}$ bodies, respectively
$O_c, O_i, O_{i,j}$	origins of the coordinate axes for bodies $B_C, B_i$ and $B_{i,j}$ , respectively
$\bar{Q}_f, \bar{Q}_r$	control effort vectors for flexible and rigid coordinates, respectively
$\bar{R}_{cm}$	position vector from the center of force to the instantaneous center of mass of the spacecraft
$\bar{R}_c, \bar{R}_i, \bar{R}_{i,j}$	position vectors of the mass elements $dm_c, dm_i$ and $dm_{i,j}$ , respectively, as measured from the center of force

$U$	potential energy of spacecraft; $U_e + U_g$
$\mathbf{U}$	unit matrix
$U_e$	strain energy of the spacecraft
$U_g$	gravitational potential energy of the spacecraft
$X_o, Y_o, Z_o$	inertial coordinate system located at the center of the earth
$X_p, Y_p, Z_p$	coordinate axes with origin at $C^f$ and parallel to $x_c, y_c, z_c$ , respectively
$X_s, Y_s, Z_s$	orbital frame with $X_s$ in the direction of the orbit-normal, $Y_s$ along the local vertical, and $Z_s$ towards the local horizontal
$\bar{\delta}_c, \bar{\delta}_i, \bar{\delta}_{i,j}$	vectors representing transverse vibration of the mass elements $dm_c, dm_i, dm_{i,j}$ , respectively
$\phi$	rotation about the local horizontal axis, $Z_1$ , of the intermediate frame $X_1, Y_1, Z_1$
$\lambda$	rotation about the local horizontal axis, $Y_2$ , of the intermediate frame $X_2, Y_2, Z_2$
$\mu_e$	gravitational constant
$\mu_{i,j}$	matrix representing slewing motion of the body $B_{i,j}$
$\theta$	true anomaly
$\theta_s, \theta_m$	slew angle and maximum slew angle, respectively
$\rho$	longitude of the ascending node
$\bar{\rho}_c, \bar{\rho}_i, \bar{\rho}_{i,j}$	vectors denoting positions of $dm_c, dm_i$ and $dm_{i,j}$ , respectively, in the undeformed configuration of the spacecraft
$\tau_s$	slewing period
$\bar{\tau}_c, \bar{\tau}_i, \bar{\tau}_{i,j}$	vectors denoting thermal

	deformations of $dm_c$ , $dm_i$ and $dm_{i,j}$ , respectively
$\omega$	argument of the perigee point
$\bar{\omega}$	librational velocity vector with respect to $X_p, Y_p, Z_p$ axes
$\psi$	rotation about the orbit normal, $X_s$

### Abrivations

**cm** : center of mass

**CMM** : Component Modes Method

**FLT** : Feedback Linearization Technique

**MSS** : Mobile Servicing System

**SMM** : System Modes Method

Dot (.) and (') represent differentiations with respect to time  $t$  and true anomaly  $\theta$ , respectively.

## Acknowledgement

I would like to thank Prof. V. J. Modi for his guidance throughout my M.A.Sc program and the preparation of the thesis as well as many other academic and nonacademic aspects.

I would like to express my appreciation to Dr. A. Ng, Dr. A. Suleman and Dr. H. Mah for their help in understanding the previous related work.

I would like to thank my wife Chao-ying for her unreserved support and understanding. Without it the completion of the thesis would have been impossible.

This project was supported by the Natural Sciences and Engineering Research Council of Canada, Grant No. A-2181; and Networks of Centers of Excellence Program, Grant No. IRIS/C-8, 5-55380. Both the grants were held by Dr. Modi.

## Chapter 1

### INTRODUCTION

#### 1.1 Preliminary Remarks

The United States, together with Canada, Japan and the European Space Agency, has committed itself to the establishment of a space station by the turn of this century. It will be used for scientific exploration, satellite launch and maintenance, manufacture of products in the favourable microgravity environment, the Earth-oriented applied technologies and numerous other applications.

The primary design requirement for the space station is to provide a versatile, expandable, permanent, manned facility for the tasks mentioned above. It will contain laboratories for a wide range of fundamental investigations. Furthermore, the space station will serve as a platform for satellite launch and repair; as well as assembly of space structures which may be too large, in terms of size and weight, to transport by the space shuttle or other launch vehicles available today.

One of the space station configurations considered by NASA is shown in Figure ( 1.1). It had a 150m long main truss (power boom), aligned with the orbit normal with eight photovoltaic arrays parallel to the local vertical, each extending to thirty-three meters and together generating 75 kW of power. The gimbaled solar array blankets provide power at any relative alignment of the space station with respect to the Sun, and heat rejection is achieved by nonrotating radiators. Habitation, laboratory and logistics modules are located near the geometric center of the power-boom. The geometry of the space

station has already gone through several modifications and, at present, its configuration is undergoing further revision. However, one thing is clear: the space station will be a gigantic and highly flexible structure. It will be the largest platform (more than 100m in length) ever assembled in space.

Such a gigantic, massive structure, however, cannot be carried in its entirety to the operational orbit. It will have to be constructed in space by integration of hardware delivered by a number of flights of the space shuttle. For instance, the the first space shuttle flight will deliver four truss bays of the power-boom, two of which are outboard of the articulating alpha joint, which allows the photovoltaic solar arrays to track the Sun. The hardware delivered will also include a radiator, two Reaction Control System (RCS) modules, fuel storage tanks for flight control and reboost, and limited avionic and communication equipment. Once assembled, it will be a fully functional spacecraft, awaiting the second shuttle flight to progress to the next stage of the assembly sequence. NASA has identified, for such an evolving structure, four milestone configurations as shown in Figure ( 1.2).

Given the large size of this orbiting system and the expected growth from the initial configuration, the structural flexibility will be a key parameter governing the space station dynamics and control. The presence of environmental and operational disturbances will only add to the complexity of the problem. Hence, thorough understanding of interactions between librational and flexible body dynamics is of importance, for the appropriate control system design, to attain the desired performance.

## 1.2 Background to the Problem

Historically, experiments with scale models have been routinely carried out to obtain useful information for the prototype design. One is, therefore, tempted to use similar

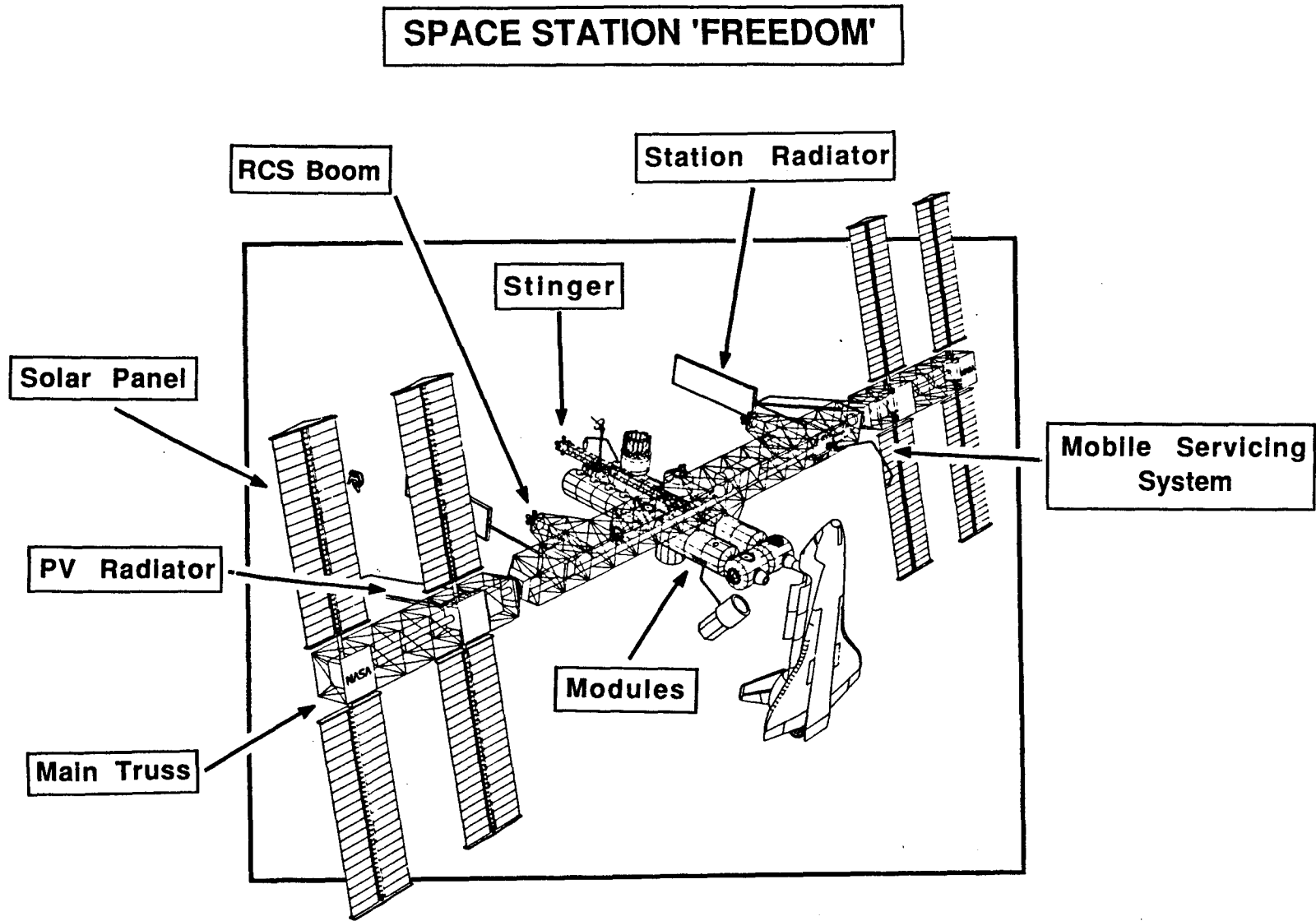


Figure 1.1: One of the earlier configurations of the proposed space station *Freedom*

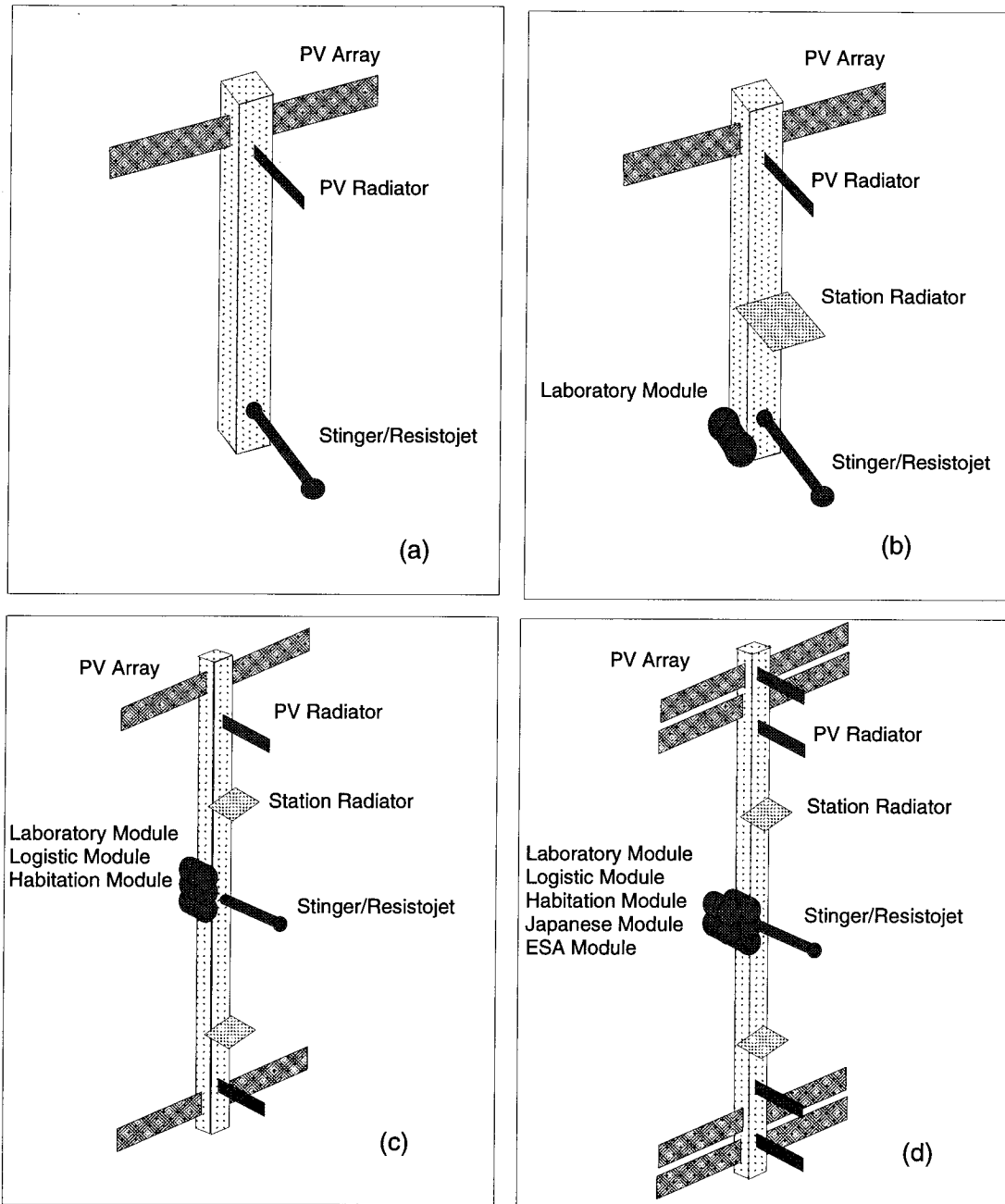


Figure 1.2: Schematic diagrams of the four milestone Configurations of the evolving space station *Freedom*: (a) First Milestone Configuration (FMC) (b) Man Tended Configuration (MTC) (c) Permanently Manned Configuration (PMC) (d) Assembly Complete Configuration (ACC).

approach for the design of space-based structures. In fact, facilities attempting to simulate some aspects of space environment have proved useful in testing of relatively small and essentially rigid spacecraft. However, ground-based experiments with large flexible space structures have been found to be of limited value due to practical difficulty in simulating environmental effects such as gravity gradient, magnetic, free molecular, microgravity, solar radiation, etc. This has led to increased dependence on numerical methods, particularly with larger, extremely elastic and complex space configurations. A general formulation applicable to a large class of systems is always attractive. Once the governing equations of motion are established and the associated integration program is operational, it becomes a powerful versatile tool.

Over the past three decades, Modi et al. as well as number of other investigators have attempted to obtain relatively general formulations for progressively complex systems to study their dynamical behaviour [1]- [8]. this has also helped in development of several linear as well as nonlinear control strategies. Of course, a number of other investigators have also approached this class of problems in a variety of different ways [9]. This has led to the generation of a vast body of literature which has been reviewed quite effectively by Modi [10] [11], Ng [12], Suleman [13], and Mah [14].

In the above mentioned developments, focus has been on the systems characterized by a large number of interconnected flexible bodies forming a tree topology. In general, dynamics of such systems is governed by a set of ‘hybrid’, nonlinear, nonautonomous and coupled equations of motion. Here ‘hybrid’ refers to the set containing both partial (elastic motion) as well as ordinary (rigid body motion) differential equations. To help obtain useful information with relative ease, it is conventional to discretize the partial differential equations into an ordinary set. This is achieved by representing the elastic deflections through a series of time dependent generalized coordinates and spatially varying admissible functions, ideally satisfying geometric and natural boundary conditions.

There are two fundamentally different choices for the admissible functions: component modes, which try to simulate the system behaviour through synthesis of the local component behavior; and system modes which attempt to accomplish the same but through the consideration of more global behaviour. Although component modes and their varied forms of synthesis have been used in practice quite widely, as shown by Suleman [13], through a simple example, there is a serious doubt as to the validity of the approach. The major problem is associated with the difficulty in satisfying complex boundary conditions in multibody systems. As future space structures are going to be highly flexible and can only be represented as interconnected multibody systems, the choice of modal functions for discretization has become an issue of enormous importance. This is understandable as validity of the dynamical response and control results depend on the accuracy of the discretization approach.

### 1.3 Scope of the Present Investigation

With this as background, the thesis aims at analyzing, understanding and hopefully arriving at better appreciation of the problem of discretization through a systematic study at a fundamental level. To begin with kinematics and kinetics of a flexible, multibody system with two levels of branching is described and the governing equations of motion obtained using the Lagrangian procedure. A computer code capable of accommodating discretization through both Component Mode Method (CMM) and System Mode Method(SMM) is developed as an extension of the contributions by Ng [12], Suleman [13] and Mah [14]. Two systems of contemporary interest are considered to asses comparative response:

- (i) two-link Mobile Flexible Manipulator(MFM) operating on a space platform;
- (ii) configuration proposed by the Control-Structure Interaction (CSI) program at NASA Langley Research Center [15].

Performance of the above two configurations is studied over a range of important system parameters to have some appreciation of the conditions leading to unacceptable performance. Finally, a control strategy, based on the Feedback Linearization Technique (FLT) accounting for the complete nonlinear dynamics of the system, is developed and its effectiveness assessed for the libration/vibration control of the above two configurations using both the discretization procedures. The thesis ends with concluding comments and recommendations for future work in this area.

Such a comparative study of discretization procedure, as applied to multibody systems with tree topology and in the presence of nonlinear control, has never been reported before.

## Chapter 2

### KINEMATICS OF THE SYSTEM

The system model is identified first and reference coordinate systems explained. This is followed by a kinematic study aimed at establishing position and velocity of an arbitrary element of the system under consideration in terms of specified and generalized coordinates.

To help study a wide variety of systems, a relatively general model of interconnected beam and plate type members, interconnected to form a tree topology, is considered in Figure ( 2.3). The system is in an arbitrary orbit about the center force, which is also the origin of the inertial reference from  $F_0$  comprised of coordinates  $X_0, Y_0, Z_0$ .  $C_f$  is the instantaneous center of mass of the system. It consists of the central body  $B_c$  to which are connected structural members  $B_i$  referred to as  $B_1, B_2, \dots, B_N$ . This may be looked upon as the first level of branching from the trunk of a tree (main body). In turn each  $B_i$  body ( $i = 1, 2, \dots, N$ ) is connected to  $B_{i,j}$  bodies ( $j = 1, 2, \dots, n_i$ ), the second level of branching. Thus the number of bodies forming the system are  $1 + N + \sum_{j=1}^N n_j$ .

The number of members  $N$  and  $n_i$  as well as their positions are kept arbitrary. Furthermore the members are free to undergo arbitrary translational and rotational maneuvers at the joints. This permits simulation of a vast variety of systems of contemporary and future interest. For instance, to simulate the proposed space station *Freedom* (present configuration which is undergoing changes), the central body  $B_c$  may simulate the main truss with the modules, stinger, radiators, photovoltaic arrays and manipulator represented by  $B_i$  and  $B_{i,j}$  bodies as shown in Figure ( 2.3)

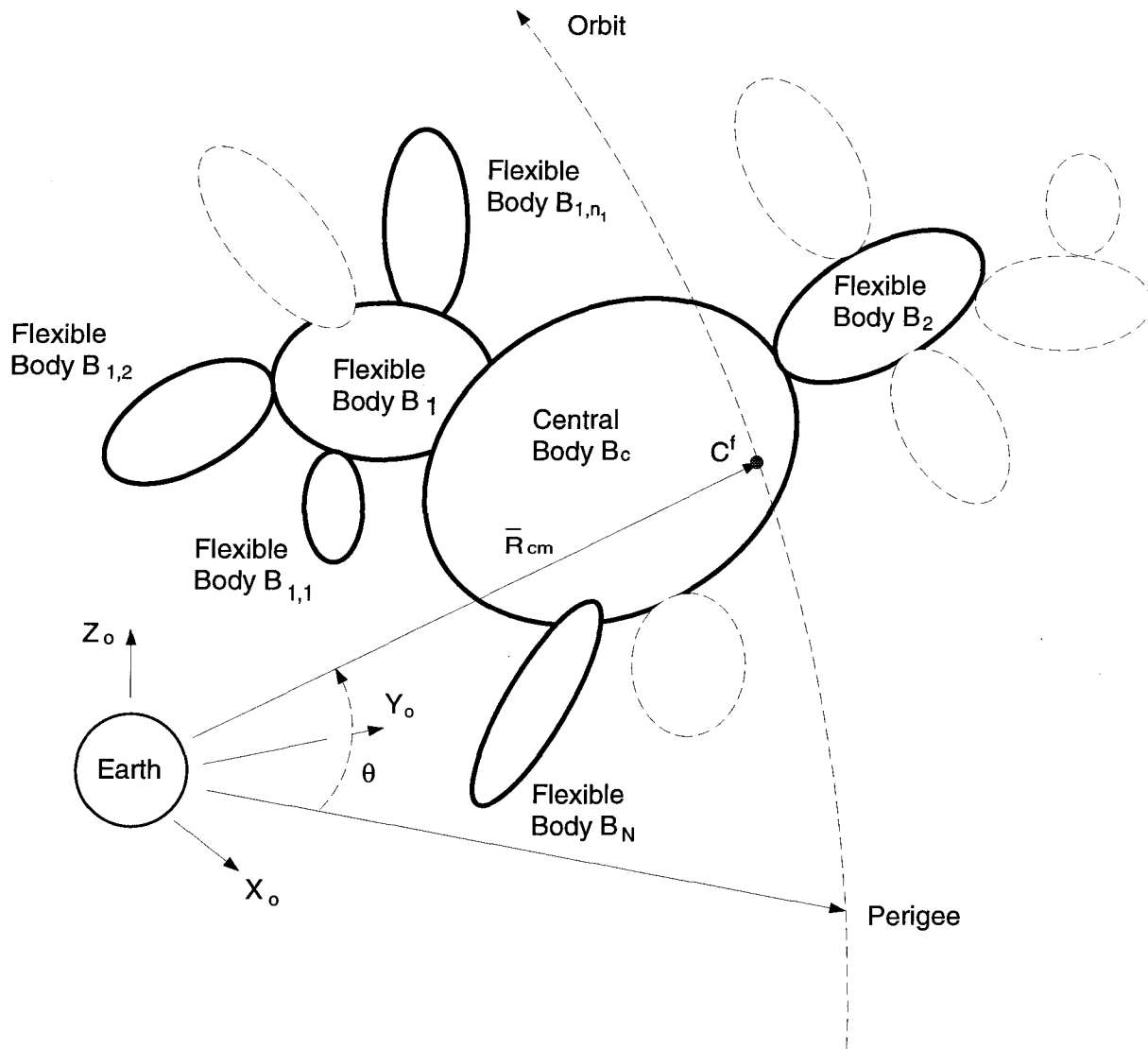


Figure 2.3: A system of interconnected bodies, forming two levels of branching, considered for study. It can represent a vast variety of systems including the proposed space station.

## 2.1 Coordinate System

Consider the system model as described before. Let  $X_0, Y_0, Z_0$  be the inertial coordinate reference located at the center of the earth. The centers of mass of undeformed and deformed configurations of the system are located at  $C^i$  and  $C^f$ , respectively. There is a body coordinate system attached to each member of the model which is helpful in defining relative motion between the members. Thus, reference frame  $F_c$  is attached to  $B_c$  at an arbitrary point  $O_c$ . Frame  $F_i$ , with origin at  $O_i$ , is attached to bodies  $B_i$  at the connecting point between body  $B_i$  and  $B_c$ . In addition, for defining attitude and solar radiation incidence angles, a reference frame is located at  $C^f$  such that the axes  $X_p, Y_p$  and  $Z_p$  are parallel to  $X_c, Y_c$  and  $Z_c$ , respectively as shown in Figure ( 2.4).

Now, an arbitrary mass element  $dm_i$  on body  $B_i$  can be reached through a direct path from  $O_c$  via  $O_i$ .  $O_c$ , in turn, is located with respect to the instantaneous center of mass  $C^f$  and the inertial reference frame  $F_o$ . Thus, the motion of  $dm_i$ , caused by librational and vibrational motions of  $B_c$  and  $B_i$ , can be expressed in terms of the inertial coordinate system. Similarly, frame  $F_{i,j}$  is attached to body  $B_{i,j}$  and has its origin at the joint between  $B_i$  and  $B_{i,j}$ . The relative position of  $O_i$  with respect to  $O_c$  is denoted by the vector  $\bar{d}_i$ , while  $\bar{d}_{i,j}$  defines the position of  $O_{i,j}$  relative to  $O_i$ .

The location of the elemental mass of the central body,  $dm_c$ , relative to  $O_c$  is defined by  $\bar{\rho}_c + \bar{\tau}_c + \bar{\delta}_c$ . Here  $\bar{\rho}_c$  indicates the undeformed position of the element;  $\bar{\tau}_c$ , the thermal deformation; and finally  $\bar{\delta}_c$  expresses the transverse vibration of the element. Similarly,  $\bar{\rho}_i, \bar{\tau}_i$  and  $\bar{\delta}_i$  define the location of the elemental mass  $dm_i$ , in body  $B_i$ , relative to  $O_i$ . For the elemental mass  $dm_{i,j}$  of body  $B_{i,j}$ , its position relative to  $O_{i,j}$  is defined by  $\bar{\rho}_{i,j}, \bar{\tau}_{i,j}$  and  $\bar{\delta}_{i,j}$ . The coordinate systems are shown in Figure (2.5).

Orientation of the coordinate axes  $X_i, Y_i, Z_i$  and  $X_{i,j}, Y_{i,j}, Z_{i,j}$  relative to  $X_c, Y_c, Z_c$  is defined by the matrices  $C_i^c$  and  $C_{i,j}^c \mu_{i,j}$ , respectively such that

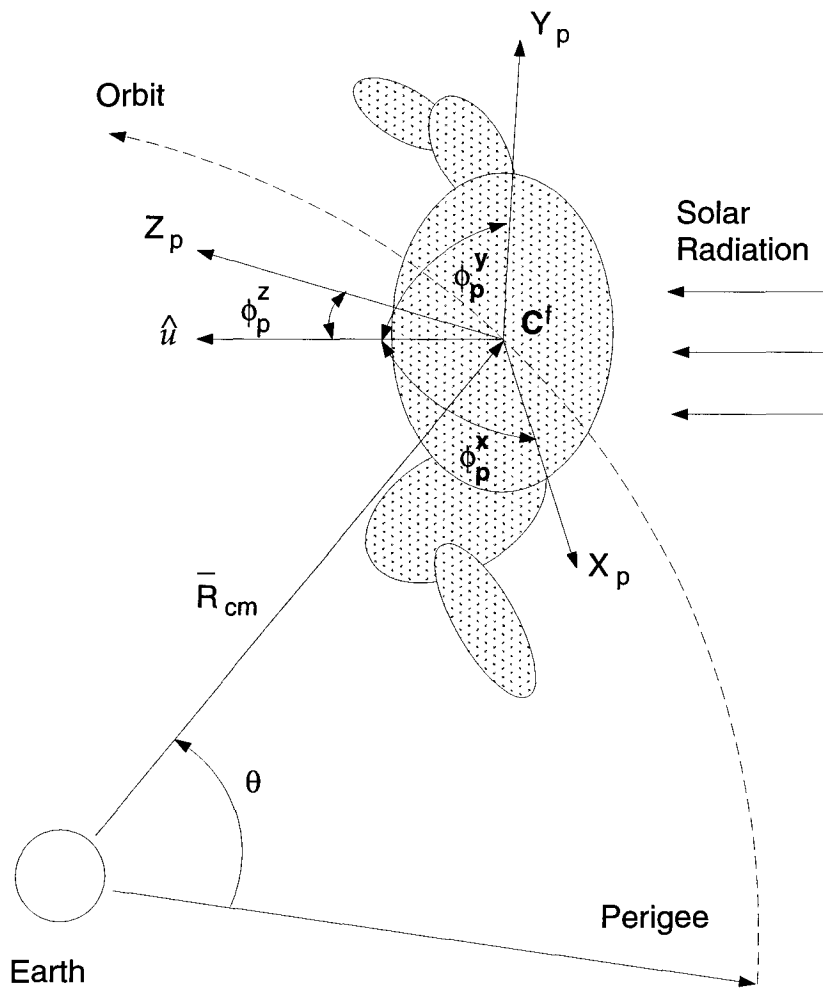


Figure 2.4: Body fixed coordinate system  $F_p(X_p, Y_p, Z_p)$  and the solar radiation incident angles.



$$\bar{u}_p = \bar{u}_c = C_i^c \mu_i = (C_{i,j}^c \mu_{i,j}) \bar{u}_{i,j}, \quad (2.1)$$

where  $\mu_{i,j}$  is the matrix denoting the motion of body  $B_{i,j}$  relative to body  $B_i$ ;  $\bar{u}_k$  ( $k = p, c, i, \text{ or } i, j$ ) is the unit column vector in the corresponding coordinate axes. For instance,  $\bar{u}_c = \{\vec{i}_c, \vec{j}_c, \vec{k}_c\}^T$ . It should be noted that the thermal deformation and transverse vibration of  $B_c$  and  $B_i$  result in the time varying characteristics of  $C_i$  and  $C_{i,j}$ , respectively.

## 2.2 Position of Spacecraft in Space

Consider an arbitrary spacecraft in orbit, as shown in Figure ( 2.6), with its instantaneous center of mass at  $C^f$ . At any instant, the position of  $C^f$  is determined by the orbital elements  $\rho, i, \omega, \epsilon, R_{cm}$  and  $\theta$ . Here  $\theta$  is the longitude of the ascending node;  $i$ , the inclination of orbit with respect to the ecliptic plane;  $\omega$ , the argument of the perigee point;  $\epsilon$ , the eccentricity of the orbit;  $R_{cm}$ , the distance from the center of the earth to  $C^f$ ; and  $\theta$ , the true anomaly of the orbit. In general,  $\rho, i, \omega$  and  $\epsilon$  are fixed while  $R_{cm}$  and  $\theta$  are considered, approximately, functions of time.

As the spacecraft has finite dimensions, i.e. it has mass as well as inertia, it is also free to undergo librational motion about its center of mass (in addition to the orbital motion). Let  $X_s, Y_s, Z_s$  represent the orbital frame with coordinates aligned along the orbit normal, local vertical, and local horizontal, respectively. Any spatial orientation of  $X_p, Y_p, Z_p$  with respect to  $X_s, Y_s, Z_s$  can be described by three modified Eulerian rotations in the following sequence: a pitch motion,  $\psi$ , about the  $X_s$ -axis giving the first set of intermediate axes  $X_1, Y_1, Z_1$ ; a roll motion,  $\phi$ , about the  $Z_1$ -axis generating the second set of intermediate axes  $X_2, Y_2, Z_2$ ; and finally a yaw motion,  $\lambda$ , about the  $Y_2$ -axis yielding  $X_p, Y_p$  and  $Z_p$ , as shown in Figure ( 2.7).

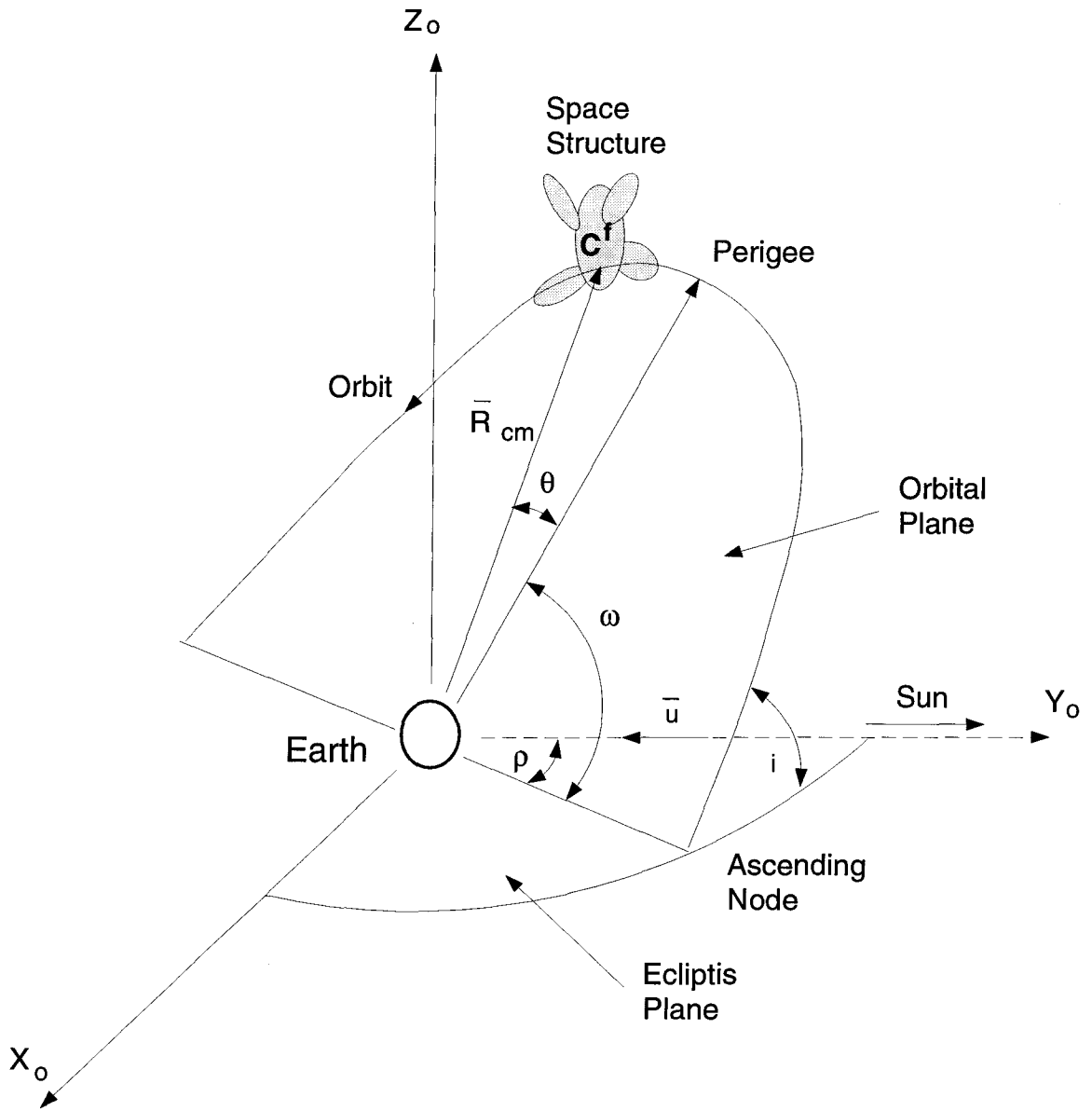


Figure 2.6: Orbital parameters for a spacecraft defining position of its center of mass.

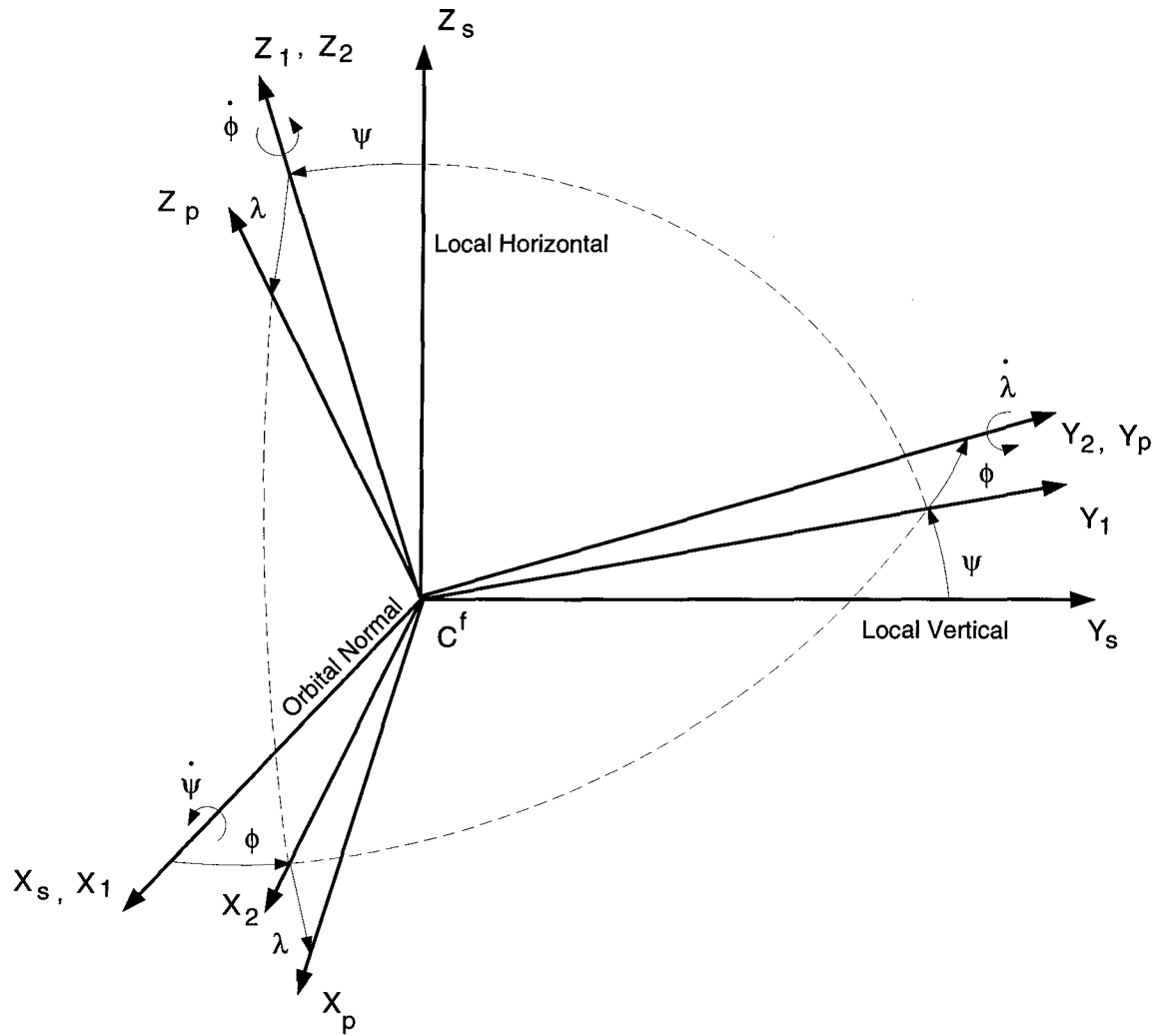


Figure 2.7: Modified Eulerian rotations specifying arbitrary orientation of the system in space.

From the system geometry and Eulerian rotations, the librational velocity vector  $\bar{\omega}$  is given by

$$\begin{aligned} \bar{\omega} = & [-\dot{\phi} \sin \lambda + (\dot{\theta} + \dot{\psi}) \cos \phi \cos \lambda] \vec{i}_p + [\dot{\lambda} - (\dot{\theta} + \dot{\psi}) \sin \phi] \vec{j}_p + \\ & + [\dot{\phi} \cos \lambda + (\dot{\theta} + \dot{\psi}) \cos \phi \sin \lambda] \vec{k}_p, \end{aligned} \quad (2.2)$$

where  $\dot{\theta}$  represents the orbital rate of the spacecraft.

### 2.3 Shift in the Center of Mass

Instantaneous position of the center of mass  $C^f$  serves as an important reference point in identifying position of the system in orbit. However, it is affected the system flexibility as well as translational and slewing motions of the appendages. Hence, determination of its position, at a given instant, is important [16] [17].

In Figure (2.5),  $C^i$  and  $C^f$  represent the centers of mass of the system during undeformed and deformed conditions, respectively. The vector  $\bar{C}_{cm}^f$ , denotes the position of  $C^f$  relative to  $C^i$ . Thus it represents the shift in the instantaneous center of mass of the spacecraft due to its deformation. This information is necessary in evaluation of the kinetic and potential energies of the system.

The vector from the origin of inertial coordinates, the center of the earth, to the mass elements  $dm_c$ ,  $dm_i$  and  $dm_{i,j}$  are denoted by  $\bar{R}_c$ ,  $\bar{R}_i$ ,  $\bar{R}_{i,j}$ , respectively. These vectors can be written as:

$$\bar{R}_c = \bar{R}_{cm} - \bar{C}_{cm}^f - \bar{C}_{cm}^i + \bar{\rho}_c + \bar{\tau}_c + \bar{\delta}_c; \quad (2.3)$$

$$\bar{R}_i = \bar{R}_{cm} - \bar{C}_{cm}^f - \bar{C}_{cm}^i + \bar{d}_i + C_i^c(\bar{\rho}_i + \bar{\tau}_i + \bar{\delta}_i); \quad (2.4)$$

$$\bar{R}_{i,j} = \bar{R}_{cm} - \bar{C}_{cm}^f - \bar{C}_{cm}^i + \bar{d}_i + C_i^c \bar{d}_{i,j} + C_{i,j}^c \mu_{i,j}(\bar{\rho}_{i,j} + \bar{\tau}_{i,j} + \bar{\delta}_{i,j}). \quad (2.5)$$

Taking moment about the center of force gives

$$\bar{R}_{cm} = \frac{1}{M} \left\{ \int_{m_c} \bar{R}_c dm_c + \sum_{i=1}^N \left[ \int_{m_i} \bar{R}_i dm_i + \sum_{j=1}^{n_i} \int_{m_{i,j}} \bar{R}_{i,j} dm_{i,j} \right] \right\}. \quad (2.6)$$

Substituting Eqs.(2.3)-(2.5) into Eq.(2.6) results in

$$\begin{aligned} \bar{C}_{cm} = \frac{1}{M} \left\{ \int_{m_c} (\bar{\rho}_c + \bar{\tau}_c + \bar{\delta}_c) dm_c + \sum_{i=1}^N \left[ \int_{m_i} \bar{d}_i + C_i^c (\bar{\rho}_i + \bar{\tau}_i + \bar{\delta}_i) dm_i \right. \right. \\ \left. \left. + \sum_{j=1}^{n_i} \int_{m_{i,j}} \bar{d}_i + C_i^c \bar{d}_{i,j} + C_{i,j}^c \mu_{i,j} (\bar{\rho}_{i,j} + \bar{\tau}_{i,j} + \bar{\delta}_{i,j}) dm_{i,j} \right] \right\}, \quad (2.7) \end{aligned}$$

where :

$$\bar{C}_{cm} = \bar{C}_{cm}^i + \bar{C}_{cm}^f$$

$\bar{C}_{cm}^i$  = position vector to  $C^i$ , the center of mass of the undeformed spacecraft, with respect to  $O_c$ ;

$\bar{C}_{cm}^f$  = position vector to  $C^f$ , relative to  $C^i$ ;

$n_i$  = number of  $B_{i,j}$  bodies attached to body  $B_i$ ;

$N$  = number of  $B_i$  bodies;

$M$  = total mass.

## 2.4 Elastic and Thermal Deformations

### 2.4.1 Background

In recent years, greater emphasis has been placed on the design of high-speed, lightweight, precision mechanical systems. These systems, in general, incorporate various types of

driving, sensing, and controlling devices working together to achieve specified performance requirements under different loading conditions.

In many of these applications, systems cannot be treated as collection of rigid bodies; i.e. flexible character of the system must be accounted for. In such cases, a mechanical system can be modeled as a collection of both rigid and flexible bodies, or an entirely flexible system depending on the situation. The flexible members may be represented as beams, plates, shells, membranes or their combinations. The design and performance analysis of such systems through dynamic simulation can be achieved provided the deformation effect is incorporated in the mathematical model.

The motion of a rigid body in the multibody system can be described by six coordinates defining its translation and rotation. They lead to a set of six independent second-order differential equations of motion.

The exact configuration of a deformable body, however, can be identified only by infinite number of coordinates. Dynamics of such continuous systems leads to a set of partial differential equations of motion which are both time- and space-dependent. To get meaningful information about the complex system behaviour, it is convenient to convert the mathematical representation into a set of ordinary differential equations by specifying deformations in terms of admissible functions of space and time dependent generalized coordinates. Admissible functions should satisfy as many natural and geometric boundary conditions as possible, and often structural modes are used to that end. However, the choice of structural modes which will converge to the right answer is still a subject of considerable controversy particularly for complex, highly flexible systems with ill-defined boundary conditions. Broadly speaking, the choice of modes can be classified into two categories leading to two different methods for studying system dynamics and control :

(i) modes defining motion of the entire system vibrating in unison, normally obtained

through finite element approach [13], referred to here as the System Mode Method (SMM);

- (ii) simpler, individual component modes appropriately synthesized to represent the system behaviour [12] called the Component Mode Method (CMM).

In the SMM, the structure is first subdivided into finite elements with degrees of freedom at the nodes. Using the local degrees of freedom as generalized coordinates, the mass and stiffness matrices of the element can be derived readily. Applying the boundary conditions for the system and compatibility requirements between adjacent elements, the system mass and stiffness matrices can be assembled from the corresponding matrices of the elements. The system modes can be evaluated numerically by using the conventional finite element method.

In the CMM, the system's flexural motion is represented in terms of the components' dynamics. The first step is to obtain the series of admissible functions, by solving the eigenvalue problem for each component, representing its elastic deformation. Next, the admissible functions are assembled so that the individual member dynamics becomes homogeneous constituent of the total system response.

#### 2.4.2 Deformation Expression for Beam-type Substructure

The governing equation for transverse vibration of a thermally fixed beam is given by

$$EI_b \frac{\partial^4 \omega^b}{\partial x^4} + \frac{\partial^2 M_t^b}{\partial x^2} + m_b \frac{\partial^2 \omega^b}{\partial t^2} = 0, \quad (2.8)$$

with the appropriate boundary conditions. As an example, for a cantilever beam fixed at  $x = 0$  and free at  $x = l_b$  the boundary conditions are:

$$\omega^b = \frac{\partial \omega^b}{\partial x} = 0, \quad \text{at } x = 0; \quad (2.9)$$

$$EI_b \frac{\partial^2 \omega^b}{\partial x^2} + M_t^b = EI_b \frac{\partial^3 \omega^b}{\partial x^3} + \frac{\partial M_t^b}{\partial x} = 0, \quad \text{at } x = l_b. \quad (2.10)$$

Here  $EI_b$  is the bending stiffness of the beam;  $m_b$ , the mass per unit length; and  $M_t^b$  the thermal bending moment given by

$$M_t^b = \int_{Area} E \alpha_f T(x, y, z) z dA; \quad (2.11)$$

where  $T(x, y, z)$  is the difference between the ambient temperature and the temperature at a point on the substructure with coordinate  $(x, y, z)$ ; and  $\alpha_f$  is the thermal expansion coefficient of the beam material. The integral is over the cross-sectional area of the substructure.

In general, a closed-form solution for the system is not available. The problem is overcome by assuming the thermal and elastic deformations to be uncoupled, i.e. the solution for thermal displacements can be obtained independent of the elastic displacements.

### 2.4.3 Thermal Deformation

The effect of thermal deformation on transient dynamics of large space structures can be significant, however, the associated analysis, in general, would be quite formidable. Fortunately, as shown by Modi and Brereton[1] the time constant of the heat balance equation is quite small, i.e. the system attains the deformed state almost instantaneously. The steady state solution shows that the shape function for a thermally flexed free-free beam is give by:

$$\frac{\delta_y}{l_b^*} = -\ln \left[ \cos \left( \frac{\eta}{l_b^*} \right) \right] \cos \phi_y; \quad (2.12)$$

$$\frac{\delta_z}{l_b^*} = -l\eta \left[ \cos \left( \frac{\eta}{l_b^*} \right) \right] \cos \phi_z; \quad (2.13)$$

where

$$l_b^* = \frac{2a_b}{\alpha_s \alpha_t q_s} \left[ \frac{k_b b_b}{a_b^2} + 4\epsilon_b \sigma_t \left( \frac{q_s \alpha_s}{\pi \epsilon_b \sigma_b} \right)^{3/4} \left( \frac{8 - \epsilon_b}{4 - \epsilon_b} \right) \right] \quad (2.14)$$

Here:

$\delta_y; \delta_z$  = deflections in the transverse Y and Z directions, respectively;

$\phi_y; \phi_z$  = solar radiation incidence angles with respect to appendage reference Y and Z directions, respectively;

$\eta$  = the distance along the appendage axis from the center point;

$l_b^*$  = the thermal reference length of the appendage. It is a function of the solar radiation intensity ( $q_s$ ), Stefa-Boltzman constant ( $\sigma_t$ ), appendage dimensions ( $a_b, b_b$ ), and appendage physical properties ( $\alpha_s, \alpha_t, \epsilon_b, k_b$ ).

Ng and Modi [18] showed that the solution to Eqs.(2.12) and (2.13) can be approximated with an error of  $\approx 3\%$  for  $\eta/l_b^* < 0.6$ :

$$\frac{\delta_y}{l_b^*} = \frac{1}{2} \left( \frac{\eta}{l_b^*} \right)^2 \cos \phi_y; \quad (2.15)$$

$$\frac{\delta_z}{l_b^*} = \frac{1}{2} \left( \frac{\eta}{l_b^*} \right)^2 \cos \phi_z. \quad (2.16)$$

Thus, for instance, the thermal deformation of a beam-type body  $B_i$  can be simulated as

$$\bar{\tau}_i = \left\{ 0, \frac{l_i^*}{2} \left( \frac{x_i}{l_i^*} \right)^2 \cos \phi_{y,i}, \frac{l_i^*}{2} \left( \frac{x_i}{l_i^*} \right)^2 \cos \phi_{z,i} \right\}^T. \quad (2.17)$$

#### 2.4.4 Transverse vibration

There are numerous possibilities for selection of the admissible functions. Consider, for example, the body  $B_c$ , a free-free beam, the admissible functions may be given by:

$$\psi^r(x) = \cosh\left(\beta^r \frac{x}{l_b}\right) + \cos\left(\beta^r \frac{x}{l_b}\right) - \gamma^r \left[ \sinh\left(\beta^r \frac{x}{l_b}\right) + \sin\left(\beta^r \frac{x}{l_b}\right) \right], \quad (2.18)$$

$$r = 1, 2, \dots;$$

where  $\beta^r l_b$  is the solution of the equation

$$\cosh(\beta^r) \cos(\beta^r) - 1 = 0; \quad (2.19)$$

and  $\gamma^r$  is given by

$$\gamma^r = \frac{\sin(\beta^r) + \sinh(\beta^r)}{-\cos(\beta^r) + \cosh(\beta^r)}. \quad (2.20)$$

For  $B_i$  and  $B_{i,j}$  treated as cantilever beams:

$$\psi^r(x) = \cosh\left(\beta^r \frac{x}{l_b}\right) - \cos\left(\beta^r \frac{x}{l_b}\right) - \gamma^r \left[ \sinh\left(\beta^r \frac{x}{l_b}\right) - \sin\left(\beta^r \frac{x}{l_b}\right) \right], \quad (2.21)$$

$$r = 1, 2, \dots;$$

where  $\beta^r$  is the solution of the equation

$$\cosh(\beta^r) \cos(\beta^r) + 1 = 0; \quad (2.22)$$

and  $\gamma^r$  is given by

$$\gamma^r = \frac{\sin(\beta^r) + \sinh(\beta^r)}{\cos(\beta^r) - \cosh(\beta^r)}. \quad (2.23)$$

## 2.5 Rotation Matrices

Matrix  $C_i^c$  appearing in Eq.(2.1) denotes orientation of the frame  $F_i$  relative to the frame  $F_c$ . Two rotation sequences are needed to determine  $C_i^c$ . The first one,  $C_i^{c;r}$ , defines

the rigid body orientation of  $F_i$  with respect to  $F_c$ ; while the second one,  $C_i^{c,f}$ , specifies rotation of the frame  $F_i$  relative to  $F'_i$  due to elastic and thermal deformations of the body  $B_c$ . The Eulerian rotations have the following sequence: rotation  $\theta_x^r$  about the  $X_c$ -axis, followed by  $\theta_y^r$  about  $Y'_c$ -axis; and finally  $\theta_z^r$  about  $Z''_c$ -axis; i.e.

$$\begin{aligned}
 C_i^{c,r} &= \begin{bmatrix} \cos \theta_z^r & -\sin \theta_z^r & 0 \\ \sin \theta_z^r & \cos \theta_z^r & 0 \\ 0 & 0 & 1 \end{bmatrix} \begin{bmatrix} \cos \theta_y^r & 0 & \sin \theta_y^r \\ 0 & 1 & 0 \\ -\sin \theta_y^r & 0 & \cos \theta_y^r \end{bmatrix} \begin{bmatrix} 1 & 0 & 0 \\ 0 & \cos \theta_x^r & -\sin \theta_x^r \\ 0 & \sin \theta_x^r & \cos \theta_x^r \end{bmatrix}, \\
 &= \begin{bmatrix} \cos \theta_y^r \cos \theta_z^r & \sin \theta_x^r \sin \theta_y^r \cos \theta_z^r - \cos \theta_x^r \sin \theta_z^r & \cos \theta_x^r \cos \theta_z^r \sin \theta_y^r + \sin \theta_x^r \sin \theta_z^r \\ \cos \theta_y^r \sin \theta_z^r & \sin \theta_x^r \sin \theta_y^r \sin \theta_z^r + \cos \theta_x^r \cos \theta_z^r & \cos \theta_x^r \sin \theta_y^r \sin \theta_z^r - \sin \theta_x^r \cos \theta_z^r \\ -\sin \theta_y^r & \sin \theta_x^r \cos \theta_y^r & \cos \theta_x^r \cos \theta_y^r \end{bmatrix}.
 \end{aligned} \tag{2.24}$$

Similarly

$$C_i^{c,f} = \begin{bmatrix} \cos \theta_y^f \cos \theta_z^f & \sin \theta_x^f \sin \theta_y^f \cos \theta_z^f - \cos \theta_x^f \sin \theta_z^f & \cos \theta_x^f \cos \theta_z^f \sin \theta_y^f + \sin \theta_x^f \sin \theta_z^f \\ \cos \theta_y^f \sin \theta_z^f & \sin \theta_x^f \sin \theta_y^f \sin \theta_z^f + \cos \theta_x^f \cos \theta_z^f & \cos \theta_x^f \sin \theta_y^f \sin \theta_z^f - \sin \theta_x^f \cos \theta_z^f \\ -\sin \theta_y^f & \sin \theta_x^f \cos \theta_y^f & \cos \theta_x^f \cos \theta_y^f \end{bmatrix}. \tag{2.25}$$

Finally,

$$C_i^c = C_i^{c,f} \times C_i^{c,r}. \tag{2.26}$$

## Chapter 3

### KINETICS OF THE SYSTEM

With the kinematics of the system established, the next logical step is to obtain the kinetic and potential energies of the system model under consideration. Application of the Lagrangian principle will then provide the equations of motion, one for each generalized coordinate, governing the system dynamics.

#### 3.1 Kinetic Energy

The kinetic energy,  $T$ , of the system is given by

$$T = \frac{1}{2} \left\{ \int_{m_c} \dot{\bar{R}}_c \dot{\bar{R}}_c dm_c + \sum_{i=1}^N \left[ \int_{m_i} \dot{\bar{R}}_i \dot{\bar{R}}_i dm_i + \sum_{j=1}^{n_i} \int_{m_{i,j}} \dot{\bar{R}}_{i,j} \dot{\bar{R}}_{i,j} dm_{i,j} \right] \right\}, \quad (3.27)$$

where  $\dot{\bar{R}}_c$ ,  $\dot{\bar{R}}_i$  and  $\dot{\bar{R}}_{i,j}$  are obtained by differentiating Eqs.(2.3)-(2.5) with respect to time:

$$\dot{\bar{R}}_c = \dot{\bar{R}}_{cm} - \dot{\bar{C}}_{cm}^f - \dot{\bar{C}}_{cm}^i + \dot{\bar{\tau}}_c + \dot{\bar{\delta}}_c + \bar{\omega} \times (-C_{cm}^f - C_{cm}^i + \bar{\rho}_c + \bar{\tau}_c + \bar{\delta}_c); \quad (3.28)$$

$$\begin{aligned} \dot{\bar{R}}_i = & \dot{\bar{R}}_{cm} - \dot{\bar{C}}_{cm}^f - \dot{\bar{C}}_{cm}^i + \dot{\bar{d}}_i + C_i^c(\dot{\bar{\tau}}_i + \dot{\bar{\delta}}_i) + \dot{C}_i^c(\bar{\tau}_i + \bar{\delta}_i) \\ & + \bar{\omega} \times [-C_{cm}^f - C_{cm}^i + \bar{d}_i + C_i^c(\bar{\rho}_i + \bar{\tau}_i + \bar{\delta}_i)]; \end{aligned} \quad (3.29)$$

$$\begin{aligned} \dot{\bar{R}}_{i,j} = & \dot{\bar{R}}_{cm} - \dot{\bar{C}}_{cm}^f - \dot{\bar{C}}_{cm}^i + \dot{\bar{d}}_i + C_i^c \dot{\bar{d}}_{i,j} \\ & + (\dot{C}_{i,j}^c \mu_{i,j} + C_{i,j}^c \dot{\mu}_{i,j})(\bar{\rho}_{i,j} + \bar{\tau}_{i,j} + \bar{\delta}_{i,j}) + C_{i,j}^c \mu_{i,j}(\dot{\bar{\tau}}_{i,j} + \dot{\bar{\delta}}_{i,j}) \\ & + \bar{\omega} \times [-C_{cm}^f - C_{cm}^i + \bar{d}_i + C_{i,j}^c \bar{d}_i + C_{i,j}^c \mu_{i,j}(\bar{\rho}_{i,j} + \bar{\tau}_{i,j} + \bar{\delta}_{i,j})]. \end{aligned} \quad (3.30)$$

Substituting Eqs.(3.28-3.30) into Eq.(3.27), the kinetic energy expression can be written in the form

$$T = T_{orb} + [T_{cm} + T_h + T_{jr} + T_t + T_v + T_{h,jr} + T_{h,t} + T_{h,v} + T_{jr,t} + T_{jr,v} + T_{t,v}] + \frac{1}{2}\bar{\omega}^T I_{sys}\bar{\omega} + \bar{\omega}^T \bar{H}_{sys}, \quad (3.31)$$

or

$$T = T_{orb} + T_{sys} + \frac{1}{2}\bar{\omega}^T I_{sys}\bar{\omega} + \bar{\omega}^T \bar{H}_{sys}, \quad (3.32)$$

where  $\bar{\omega}$  is the librational velocity vector;  $I_{sys}$ , the inertia matrix;  $\bar{H}_{sys}$ , the angular momentum with respect to the  $F_c$  frame;  $\frac{1}{2}\bar{\omega}^T I_{sys}\bar{\omega}$ , the kinetic energy due to pure rotation; and  $\bar{\omega}^T \bar{H}_{sys}$ , the kinetic energy due to coupling between the rotational motion, transverse vibration, and thermal deformation.  $T_{sys}$  represents the kinetic energy contributions due to various other effects contributed by flexibility, shift in the center of mass and associated coupling terms. The subscripts involved are as follows:

$orb$  = orbital motion;

$cm$  = centre of mass motion;

$h$  = hinge position between body  $B_c$  and  $B_i$  or between body  $B_i$  and  $B_{i,j}$ ;

$jr$  = joint rotation due to elastic and thermal deformation;

$t$  = thermal deformation;

$v$  = transverse vibration.

For instance ,  $T_{t,v}$  refers to the contribution of kinetic energy due to the rate of thermal deformation and transverse vibration velocity. Details of the kinetic energy expression are given in Appendix A.

$I_{sys}$  and  $H_{sys}$  represent the inertia and angular momentum vectors of the system, respectively. They are time dependent and can be given by:

$$I_{sys} = I_{cm} + I_h + I_r + I_t + I_v + I_{h,r} + I_{h,t} + I_{h,v} + I_{r,t} + I_{r,v} + I_{t,v}; \quad (3.33)$$

$$\begin{aligned} \bar{H}_{sys} = & \bar{H}_{cm} + \bar{H}_h + \bar{H}_{j,r} + \bar{H}_t + \bar{H}_v + \bar{H}_{h,jr} + \bar{H}_{h,r} + \bar{H}_{h,t} + \bar{H}_{h,v} \\ & + \bar{H}_{r,t} + \bar{H}_{r,v} + \bar{H}_{t,v}. \end{aligned} \quad (3.34)$$

Here subscript  $r$  denotes contribution from the rigid body components. The details of  $I_{sys}$  and  $H_{sys}$  are also given in Appendix A.

### 3.2 Potential Energy

The potential energy ,  $U$ , of the system has two sources: gravitational potential energy,  $U_g$ ; and strain energy,  $U_e$ , due to transverse vibration and thermal deformation,

$$U = U_e + U_g. \quad (3.35)$$

The potential energy due to the gravity gradient is given by

$$U_g = \mu_e \left\{ \int_{m_c} \frac{dm_c}{R_c} + \sum_{i=1}^N \left[ \int_{m_i} \frac{dm_i}{R_i} + \sum_{j=1}^{n_i} \int_{m_{i,j}} \frac{dm_{i,j}}{R_{i,j}} \right] \right\}. \quad (3.36)$$

Substituting the expressions for  $R_c$ ,  $R_i$  and  $R_{i,j}$  from Eqs.(2.3)-(2.5) and neglecting the terms of order  $1/R_{cm}^4$  and higher,  $U_g$  can be written as

$$U_g = -\frac{\mu_e M}{R_{cm}} - \frac{\mu_e}{2R_{cm}^3} trans[I_{sys}] + \frac{3\mu_e}{2R_{cm}^3} \bar{l}^T I_{sys} \bar{l}, \quad (3.37)$$

where  $\mu_e$  is the gravitational constant and  $\bar{l}$  represents the direction cosine vector of  $\bar{R}_{cm}$  with respect to the  $X_p, Y_p, Z_p$  axis,

$$\begin{aligned} \bar{l} = & (\cos \psi \sin \phi \cos \lambda + \sin \psi \sin \lambda) \bar{i}_c + \cos \psi \cos \phi \bar{j} - c \\ & (\cos \psi \sin \phi \sin \lambda - \sin \psi \cos \lambda) \bar{k}_c. \end{aligned} \quad (3.38)$$

The strain energy expression for a beam is

$$U_{e,beam} = \frac{1}{2} \int_{l_b} \left\{ EI_{yy} \left( \frac{\partial^2 \omega^b}{\partial x^2} \right)^2 + ETI_{zz} \left( \frac{\partial^2 \nu^b}{\partial x^2} \right)^2 \right\} dl_b, \quad (3.39)$$

where  $EI_{yy}$  and  $EI_{zz}$  are the bending stiffnesses of the beam about the  $Y$  and  $Z$  axes, respectively.

### 3.3 Equations of Motion

Using the Lagrangian procedure, the equation of motion can be obtained from

$$\frac{d}{dt} \left( \frac{\partial T}{\partial \dot{q}} \right) - \frac{\partial T}{\partial q} + \frac{\partial U}{\partial q} = F_q, \quad (3.40)$$

where  $q$  and  $F_q$  are the generalized coordinates and generalized forces, respectively. Normally, the effect of librational and vibrational motions on the orbital trajectory is small. Hence, the orbit can be expressed by the classical Keplerian relations:

$$R_{cm} = \frac{h^2}{\mu_e (1 + \epsilon \cos \theta)}; \quad (3.41)$$

$$R_{cm}^2 \dot{\theta} = h; \quad (3.42)$$

where  $h$  is the angular momentum per unit mass of the system;  $\mu_e$  is the gravitational constant; and  $\epsilon$  is the eccentricity of the orbit. The general form of the equations of motion can be written as

$$\begin{bmatrix}
 & & \vdots & & \\
 & M_r & \vdots & M_{r,f} & \\
 & & \vdots & & \\
 \dots & \dots & \dots & \dots & \dots \\
 & & \vdots & & \\
 M_{f,r} & & \vdots & M_f & \\
 & & \vdots & & 
 \end{bmatrix}
 \begin{bmatrix}
 \psi'' \\
 \phi'' \\
 \lambda'' \\
 \dots \\
 q_1'' \\
 \vdots \\
 q_{n_v}''
 \end{bmatrix}
 +
 \begin{bmatrix}
 C_\psi \\
 C_\phi \\
 C_\lambda \\
 \dots \\
 C_{q_1} \\
 \vdots \\
 C_{q_{n_v}}
 \end{bmatrix}
 +
 \begin{bmatrix}
 K_\psi \\
 K_\phi \\
 K_\lambda \\
 \dots \\
 K_{q_1} \\
 \vdots \\
 K_{q_{n_v}}
 \end{bmatrix}
 =
 \begin{bmatrix}
 Q_\psi \\
 Q_\phi \\
 Q_\lambda \\
 \dots \\
 Q_{q_1} \\
 \vdots \\
 Q_{q_{n_v}}
 \end{bmatrix}, \tag{3.43}$$

or

$$\mathbf{M}(\mathbf{q})\bar{\mathbf{q}}'' + \bar{\mathbf{C}}(\mathbf{q}, \mathbf{q}', \theta) + \bar{\mathbf{K}}(\mathbf{q}, \theta) = \bar{\mathbf{Q}}(\theta), \tag{3.44}$$

where primes denote differentiation with respect to the true normaly  $\theta$ . Note,  $n_v$  represents the number of vibrational degrees of freedom. Hence, the total number of generalized coordinates  $N_q$  equals the three librational coordinates  $\psi, \phi, \lambda$  plus  $n_v$ .  $M$  is a nonsingular asymmetric matrix of dimension  $N_q \times N_q$ . The entries in  $M$  come from the second order terms of  $d/d\theta(\partial T/\partial q')$ .  $\bar{C}$  is a  $N_q \times 1$  vector. The terms here are derived from two sources: Coriolis contribution of  $d/d\theta(\partial T/\partial q')$ ; and from  $\partial T/\partial q'$ .  $\bar{K}$ , also a  $N_q \times 1$  vector, denotes the stiffness of the system. It is composed of the terms from  $\partial U/\partial q$ .  $\bar{Q}$ , the generalized force vector of dimension  $N_q \times 1$ , is evaluated using the virtual work principle. Nonlinear entries in  $M$  together with nonlinear and time varying components of  $\bar{C}$ ,  $\bar{K}$  and  $\bar{Q}$  result in a set of coupled, nonlinear and nonautonomous equations of motion.

As pointed out before, the equations of motion are applicable to a wide variety of systems because of the relatively general character of the model. They range from communication satellites to the evolving space station *Freedom* and robotic manipulators,

to mention a few configurations of current interest. More important features of the formulation may be summarized as follows:

- (i) It is applicable to an arbitrary number of beam, plate and rigid body members, in any desired orbit, interconnected to form an open branch-type topology.
- (ii) Joints are provided with translational and rotational degrees of freedom. For example, in the Space Station configuration, the solar panels can undergo predefined slewing and translational maneuvers with respect to the central body, to track the Sun for optimal power production.
- (iii) The formulation accounts for the effects of transient system inertias, shift in the center of mass, geometric nonlinearities, shear deformations and rotary inertias. It also considers solar radiation induced thermal effects. Thus it is possible to study the complex system dynamics involving interactions between librational motion, transverse vibrations and thermal deformations.
- (vi) Environmental forces (aerodynamic, magnetic, etc.) and operational disturbances (Orbiter docking, EVA activity, etc.) can be incorporated readily through generalized forces and initial conditions.
- (v) The governing equations are programmed in a modular fashion to isolate the effects of slewing , librational dynamics, flexibility, orbital parameters, etc.
- (vi) The equations are amenable to discretization using both component as well as system modes thus facilitating comparison between their relative merit.
- (vii) The equations of motion can be cast, quite readily, into a form suitable for both linear and nonlinear control studies.

## Chapter 4

### AN APPROACH TO CONTROL

A system is usually designed according to prescribed specifications to achieve a desired level of performance. Besides performing the required tasks efficiently, it must also exhibit several desirable properties such as stability, quick response, disturbance rejection, etc. For flexible space based systems, governed by highly nonlinear, nonautonomous and coupled equations of motion, this is possible only in the presence of active control. Misawa and Hedrick [19] have reviewed the pertinent literature at some length.

As can be expected, the control strategy can vary rather widely. There are literally thousands of control algorithms written to meet a variety of situations and performance requirements. More recent approaches include extended linearization [20],[21]; feedback linearization [22]-[24] or, in simplified cases, the inverse control [25] and several others [26]-[32].

In the present study, the Feedback Linearization Technique (FLT), which completely accounts for the system's nonlinear dynamics, is used to control large, flexible, multibody structures in space.

#### 4.1 Feedback Linearization Technique (FLT)

Feedback linearization is an approach for the nonlinear control system design . The basic idea is to algebraically transform the nonlinear system dynamics into an equivalent uncoupled canonical form (partly or fully ) so that linear control techniques can be applied.

It also can be used as a model-simplifying method in the development of robust or adaptive nonlinear controllers. In its simplest form, the FLT amounts to cancellation of the nonlinearities so that the closed-loop dynamics is in a linear form. It is applicable to a class of nonlinear systems described by the so-called companion form, or the controllability canonical form. A system is said to be in the companion form if its dynamics is represented by

$$\dot{x}^{(n)} = f(x) + b(x)u, \quad (4.45)$$

where  $u$  is the scalar control input;  $x$  is the scalar output of interest with  $\bar{x} = [x, \dot{x}, \dots, x^{(n)}]^T$  as the state vector; and  $f(x)$ , a nonlinear function of the states. Note, in the state-space representation, Eq.(4.45) can be written as

$$\frac{d}{dt} \begin{bmatrix} x_1 \\ \vdots \\ x_{n-1} \\ x_n \end{bmatrix} = \begin{bmatrix} x_2 \\ \vdots \\ x_n \\ f(x) + b(x)u \end{bmatrix}. \quad (4.46)$$

Using the control input (assuming  $b$  to be non-zero) for the systems which can be expressed in the controllability canonical form,

$$u = \frac{1}{b}[v - f]. \quad (4.47)$$

One can cancel the nonlinearities and obtain the simple input-output relation (multiple-integrator form )

$$\dot{x}^{(n)} = v, \quad (4.48)$$

with the control law

$$v = -k_1 x_1 - k_2 x_2 - \dots - k_{n-1} x^{n-1}, \quad (4.49)$$

where the  $k_i$ 's are chosen so that  $p^n + k_{n-1}p^{n-1} + \dots + k_1$  is a stable polynomial. At the same time, one can place the poles at the desired locations, i.e. reaching the pole-placement target. This leads to an exponentially stable dynamics,

$$x^{(n)} + k_{n-1}x^{(n-1)} + \dots + k_1 x = 0, \quad (4.50)$$

which implies that  $x(t) \rightarrow 0$ .

For the tasks involving tracking of a desired output  $x_d(x)$ , the control law

$$u = x_d^{(n)} - k_1 e - k_2 \dot{e} - \dots - k_{n-1} e^{(n-1)}, \quad (4.51)$$

with  $e = x(t) - x_d(t)$  as the tracking error, leads to the exponentially convergent tracking. Note, similar results would be obtained if the scalar  $x$  was replaced by a vector and the scalar  $b$  by an invertible square matrix.

When the nonlinear dynamics is not in the controllability canonical form, one may have to use transformations to arrive the form before using the above mentioned feedback linearization approach. At times, only partial linearization of the original dynamics is possible. Consider a system as

$$\dot{x} = f(x, u). \quad (4.52)$$

Let us apply the technique referred to as input-state linearization. There are two steps involved. First, one finds a state transformation  $Z = w(x)$  and a input transformation  $U = g(x, v)$  so that the nonlinear system dynamics is transformed into that of an equivalent linear system. Next, one may use a standard linear technique (such as the

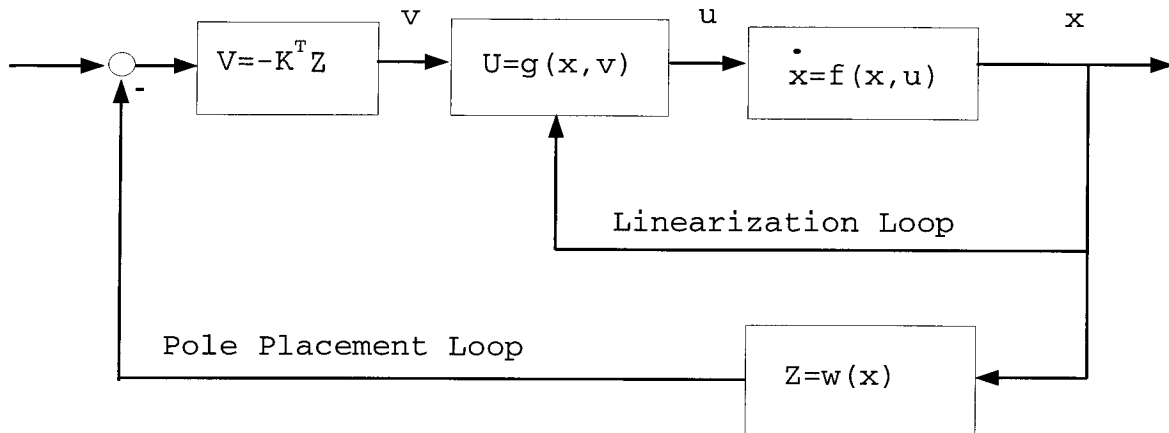


Figure 4.8: Block diagram of a feedback linearized control system

pole placement) to design the equivalent input  $v$ . The block diagram for the procedure is presented in Figure (4.8).

Following remarks can be made about the method:

- (i) The result is valid in a large region of the state space except for the singularities.
- (ii) The technique involves combination of the state transformation as well as the input transformation, with the state feedback in both. Thus, it is a linearization by feedback and hence the designation Feedback Linearization Technique. This is fundamentally different from the Jacobian linearization for a small range operation which is the basis for linear control.
- (iii) In order to implement the control law, the new state components ( $Z$ ) must be available. They must be physically meaningful, measurable and amenable to determination from  $Z=w(x)$ .
- (iv) In general, one relies on the system model for both the controller design and the

computation . If there is an uncertainty in the model, it will lead to errors in the computation of both the new state  $Z$  and the control input  $U$ .

- (v) Tracking control can also be considered. However, the desired motion then needs to be expressed in terms of the complete new state vector. Complex computations may be involved in transforming the desired motion specifications ( of physical output variables ) into specifications in terms of the new state.

## 4.2 Control Implementation Procedures

As shown in Chapter 3 , dynamics of a flexible spacecraft with  $\bar{q}_r$  and  $\bar{q}_f$  corresponding to librational and vibrational generalized coordinates, respectively, is given by

$$\begin{bmatrix} M_{r,r} & M_{r,f} \\ M_{f,r} & M_{f,f} \end{bmatrix} \begin{Bmatrix} \ddot{\bar{q}}_r \\ \ddot{\bar{q}}_f \end{Bmatrix} + \begin{Bmatrix} \bar{F}_r \\ \bar{F}_f \end{Bmatrix} = \begin{Bmatrix} \bar{Q}_r \\ \bar{Q}_f \end{Bmatrix}. \quad (4.53)$$

Here  $M_{r,r}$  is a  $3 \times 3$  matrix for the librational degrees of freedom;  $M_{r,f}$  is a  $3 \times (N_q - 3)$  matrix, representing coupling between the rigid and flexible generalized coordinates;  $M_{f,r} = M_{r,f}$ ; and  $M_{f,f}$  is a  $(N_q - 3) \times (N_q - 3)$  submatrix for the flexible degrees of freedom.  $\bar{F}_r$  and  $\bar{Q}_r$  are  $3 \times 1$  vectors representing the first and second order coupling terms and the generalized force for the rigid part of the system, respectively. Similarly,  $\bar{F}_f$  and  $\bar{Q}_f$  are  $(N_q - 3) \times 1$  vectors corresponding to the first and second order coupling terms and generatized force for the flexible part of the system, respectively. Assuming only the generalized coordinates of the librational degrees of freedom to be observable, the control force  $\bar{Q}_f$  is not applicable and hence set to zero. The objective is to determine the control input  $\bar{Q}_r$  such that the closed-loop system is linearized and has desired pole-positions. Consistent with the assumption:

$$M_{rr}\ddot{\bar{q}}_r + M_{rf}\ddot{\bar{q}}_f + \bar{F}_r = \bar{Q}_r; \quad (4.54)$$

$$M_{fr}\ddot{\bar{q}}_r + M_{ff}\ddot{\bar{q}}_f + \bar{F}_f = 0; \quad (4.55)$$

which can be solved for  $\ddot{\bar{q}}_r$  and  $\ddot{\bar{q}}_f$  as:

$$\bar{M}\ddot{\bar{q}}_r + \bar{F} = \bar{Q}_r; \quad (4.56)$$

$$\ddot{\bar{q}}_f = -M_{ff}^{-1}M_{fr}\ddot{\bar{q}}_r - M_{ff}^{-1}\bar{F}_f; \quad (4.57)$$

where:

$$\bar{M} = M_{rr} - M_{rf}M_{ff}^{-1}M_{fr}; \quad (4.58)$$

$$\bar{F} = \bar{F}_R - M_{rf}M_{ff}^{-1}\bar{F}_f. \quad (4.59)$$

Fortunately, the system has the controllability canonical form. A suitable choice for  $Q_r$  would be

$$\bar{Q}_r = \bar{M}\bar{v} + \bar{F}, \quad (4.60)$$

with

$$\bar{v} = (\ddot{\bar{q}}_r)_d + K_v[(\dot{\bar{q}}_r)_d - \dot{\bar{q}}_r] + k_p[(\bar{q}_r)_d - \bar{q}_r]. \quad (4.61)$$

Now the controlled equations of motion become:

$$\ddot{\bar{q}}_r = \bar{v}; \quad (4.62)$$

$$\ddot{\bar{q}}_f = -M_{ff}^{-1}M_{fr}\bar{v} - M_{ff}^{-1}\bar{F}_f. \quad (4.63)$$

Here:  $\bar{Q}_r = \bar{M}(\ddot{\bar{q}}_r)_d + \bar{F} + \bar{M}(K_v \dot{e} + K_p e)$ ; and  $e = (q_r)_d - q_r$  is the error between desired output and the system output . The controller is composed of two parts: the primary controller  $\bar{Q}_{r,p} = \bar{M}(\ddot{\bar{q}}_r)_d + \bar{F}$ ; and the secondary controller:  $\bar{Q}_{r,s} = \bar{M}(k_v \dot{e} + k_p e)$ .

The quasi-closed loop control block diagram is shown in Figure (4.9). Note, the controller solves the tracking, stability and linearization problems at the same time. As shown in Chapter 6, the control strategy improves the system behaviour significantly.

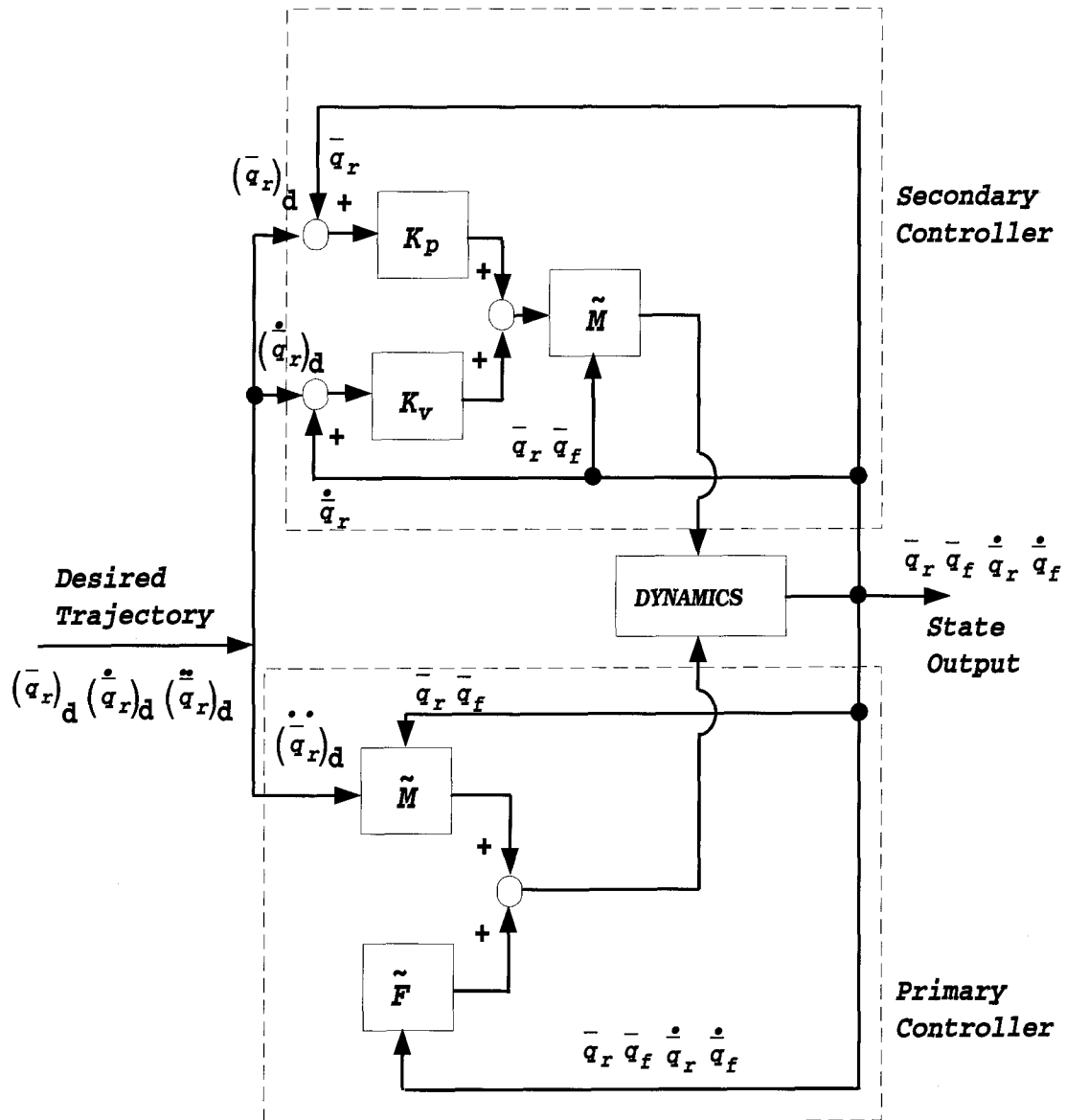


Figure 4.9: Block diagram of the Quasi-closed loop control system

## Chapter 5

### COMPUTATIONAL CONSIDERATIONS

As pointed out before, formulation of the problem for dynamical and control studies of a multibody system, comprised of rigid bodies, beam and plate type members is a challenging task. The governing equations were found to be extremely lengthy (even in the matrix form), highly nonlinear, nonautonomous, and coupled. Equally formidable is the development of an efficient numerical code for their integration. This chapter briefly indicates approach used to this end. Modular nature to help isolate influence of various system parameters as well as user friendliness were the two characteristic features which guided the process. Depending on the discretization process used, two separate programs were required.

#### 5.1 Program Structure of the Component Modes Method (CMM)

The overall program is composed of several stages or phases. The first one is the input phase, followed by numerical integration, output part and completion test. It is schematically shown in Figure (5.10). The input phase includes:

- (i) orbital parameters  $\rho, i, \omega$  and eccentricity  $\varepsilon$ ;
- (ii) program control parameters, simulation period, numerical integration tolerance, initial step-size, and output data;
- (iii) initial conditions of the state variables.

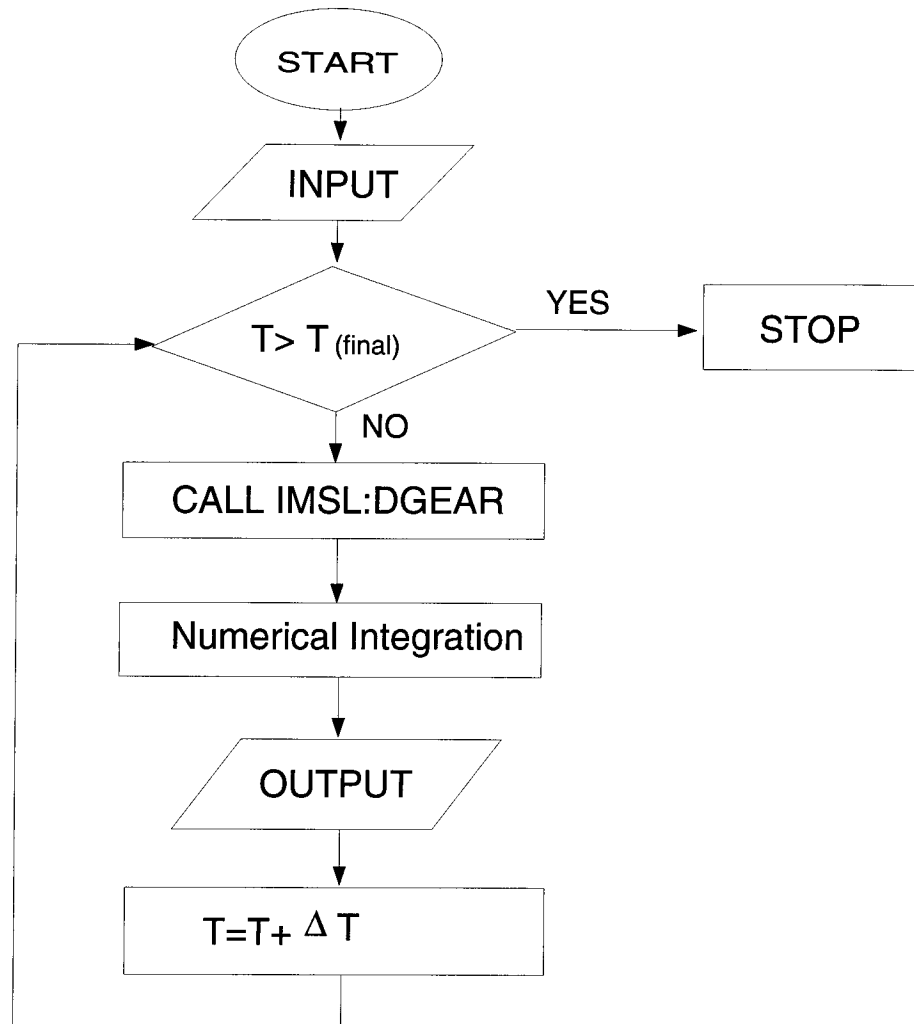


Figure 5.10: Program flow-chart for the CMM simulation

Two data files used are referred to as MODEL and MODE. They are described in the Appendix B.

The method DGEAR was chosen to perform the numerical integration of the equations of motion. This is a mature method. In most cases, it is robust. Also it can automatically adjust the integration step-size and select appropriate iteration procedure.

FCN block calculates the right function values, e.g. value of the the state vector at the time of  $T + \Delta T$ . Here  $\Delta T$  is the time step-size used by the DGEAR at the instant. Output and completion test-blocks are determined by the input data file. They are used to output the data in a proper format and stop the simulation at a chosen time, respectively. The numerical integration flowchart is presented in Figure (5.11).

## 5.2 Program Structure for the System Modes Method (SMM)

The first step is to obtain system modes using the finite element method. Thus the program has two major parts: the finite element module; and the dynamic analysis module. They are presented in Figure (5.12) and (5.13), respectively. Updating of the system modes for spacecraft with time dependent geometries, such as rotating solar panels or slewing robotic arms, cannot be overemphasized. System modes reflect elastic character of the entire spacecraft, hence their variation with the geometry can affect the system response significantly. There is an important decision to be made: how often to update the system modes? Obviously one has to strike a balance between the available computational resources, need for real-time information and accuracy. Long updating time may lead to discontinuity in response, which may not be acceptable. Of course, by frequent updating one can avoid such problem, however, only at a considerable computational cost.

The input I block in Figure (5.12) introduces material properties of the structure

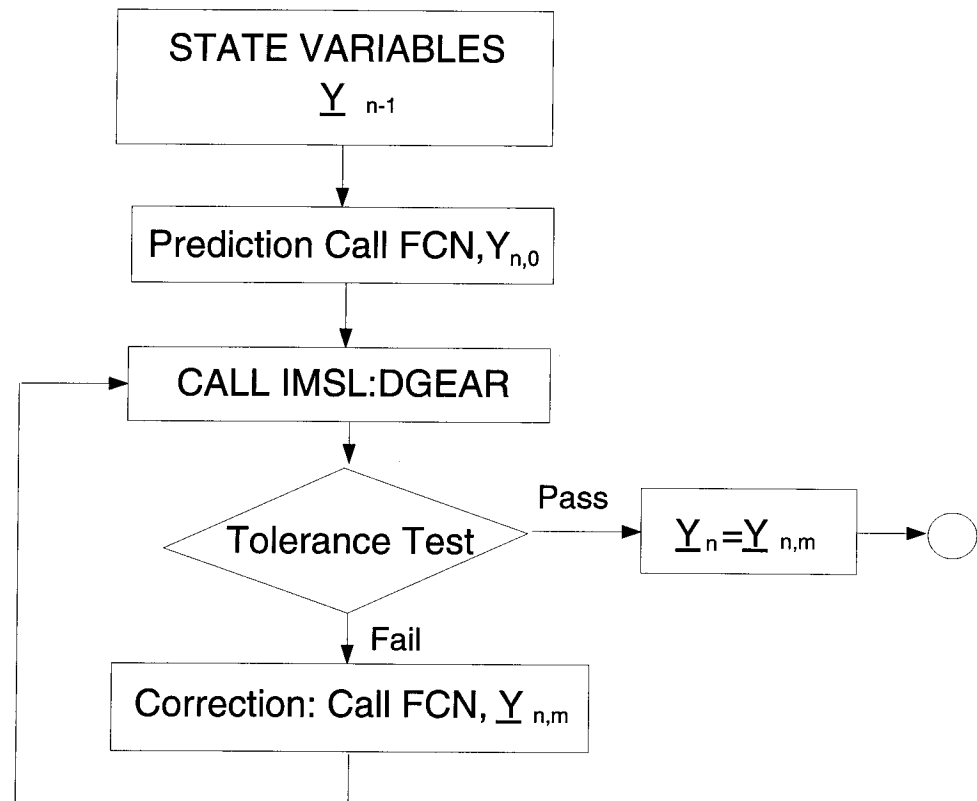


Figure 5.11: Flow-chart showing the numerical integration procedure using the CMM

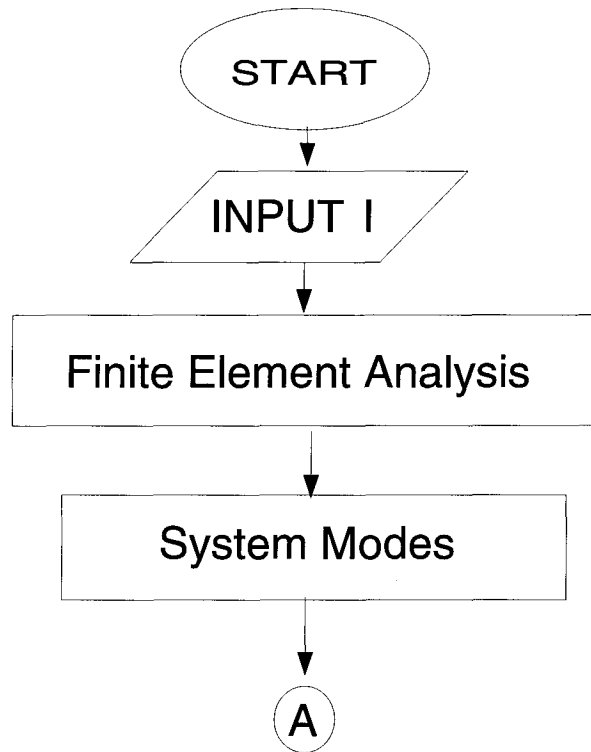


Figure 5.12: Program flow-chart for the system modes determination.

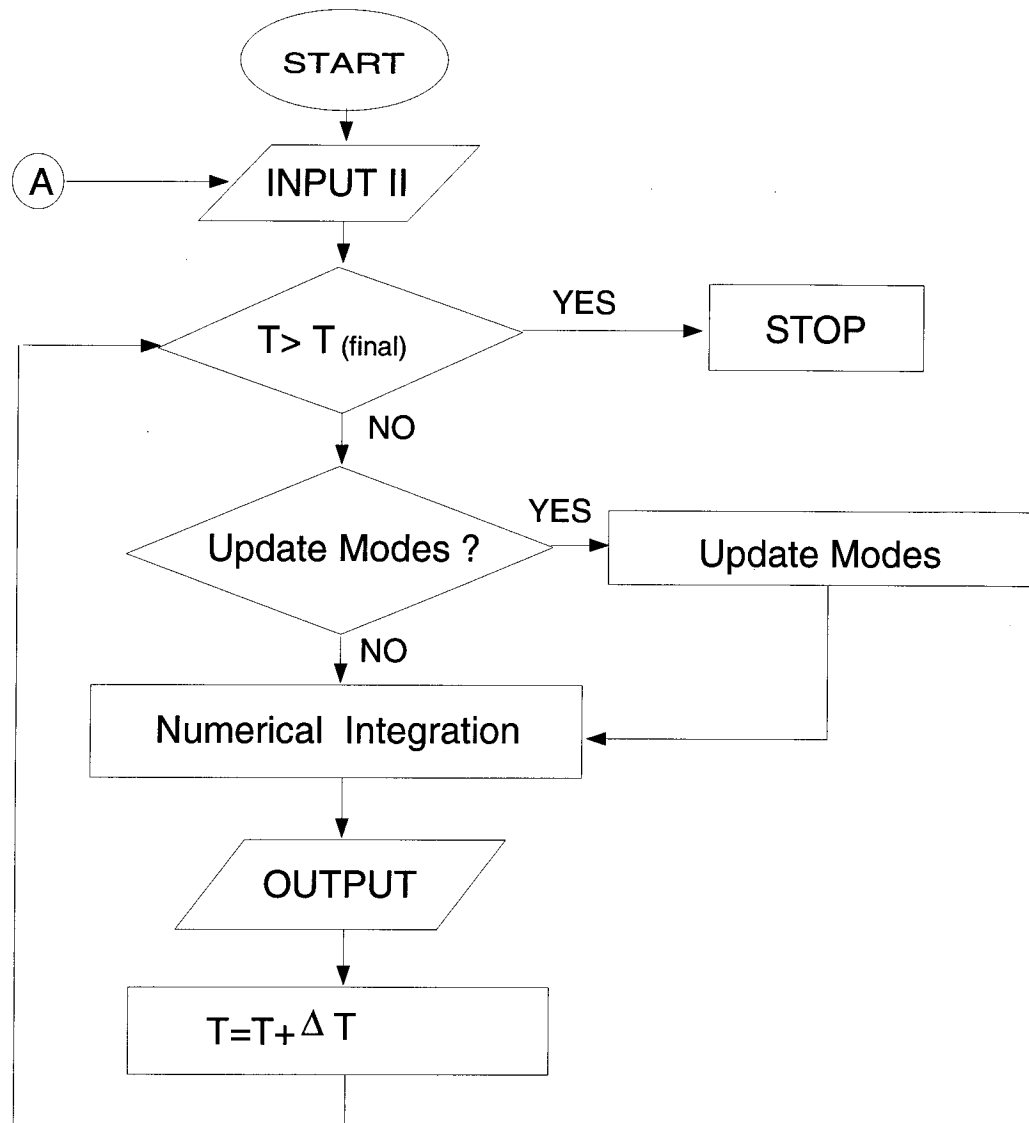


Figure 5.13: Program flow-chart for the SMM simulation

necessary for calculation of the system modes. Input II, in Figure (5.13), enters the simulation period, numerical integration and program control parameters, mode update information, etc. Details of the input files are presented in the Appendix C.

## Chapter 6

### RESULTS AND DISCUSSION

#### 6.1 Two Link Mobile Servicing System

With the formulation applicable to a class of multibody systems in hand and the associated computer code operational, the next logical step is to illustrate its effectiveness. To that end two different configurations of contemporary interest are considered:

- (i) a two-arm, mobile, flexible manipulator operating on a rigid platform;
- (ii) NASA proposed system for Control-Structure-Interaction(CSI) study.

There are three basic objectives:

- (i) potential to undertake parametric studies if desired;
- (ii) effectiveness of the FLT for control accounting for the complete nonlinear system dynamics;
- (iii) relative merit of the system and component modes discretization.

It is not intended here to generate a vast body of results for each of the systems under consideration. Of course the code can provide the information as desired by spacecraft designers. The objective is primarily to show the potential of this powerful versatile tool.

The proposed space station *Freedom*, expected to be operational by the turn of the century, will support a Mobile Servicing System (MSS). It is essentially a two link manipulator on a mobile base which can traverse along the main truss of the station treated as a

Table 6.1: Numerical values used in simulation of the two-link manipulator

	M (kg)	L (m)	$\omega$ (rad/s)	$I_{xx}$ (kgm <sup>2</sup> )	$I_{yy}$ (kgm <sup>2</sup> )	$I_{zz}$ (kgm <sup>2</sup> )
Center Body	240,120	115.35	rigid	$8 \times 10^5$	$2.67 \times 10^8$	$2.67 \times 10^8$
Upper Link	1,800	7.5	0.167	101	33,750	33,750
Lower Link	1,800	7.5	0.167	101	33,750	33,750

free-free beam. The system is expected to be the workhorse for the station's construction, maintenance, operation, and future evolution.

The objective of the simulation here is to assess:

- (a) effect of the more important system parameters on the response;
- (b) effectiveness of the nonlinear feedback linearization control.

The system geometry is shown in Figure (6.14) with the numerical values used in the simulation presented in Table (6.1). The slewing maneuver of the manipulator is taken to be a sine-ramp function thus resulting in zero velocity and acceleration at the beginning and end of the operation:

$$\theta_s = \begin{cases} \theta_m \cdot (\tau/\tau_s) - (\theta_m/2\pi) \sin(2\pi\tau/\tau_s), & \tau \leq \tau_m \\ \theta_m & \tau > \tau_m. \end{cases} \quad (6.64)$$

Here:  $\theta_s$ , slew angle at an instant  $\theta$  (true anomaly);  $\theta_m$ , maximum slew angle; and  $\tau_s$ , duration of the slew. To help isolate the effect, only the lower arm was considered to undergo the specified slewing motion in the plane of the orbit. Also only the first cantilever mode is used to represent the link flexibility. The space station is taken to be rigid although the formulation and the program accounts for its flexibility.

Figure (6.15) shows the effect of increasing the magnitude as well as speed of the slewing maneuver. Three cases are considered corresponding to the slewing magnitude of 45°, 90° and 180° completed in 10 minutes with the manipulator located at the center of the station. Note, the inplane maneuver excites only the pitch librational motion,

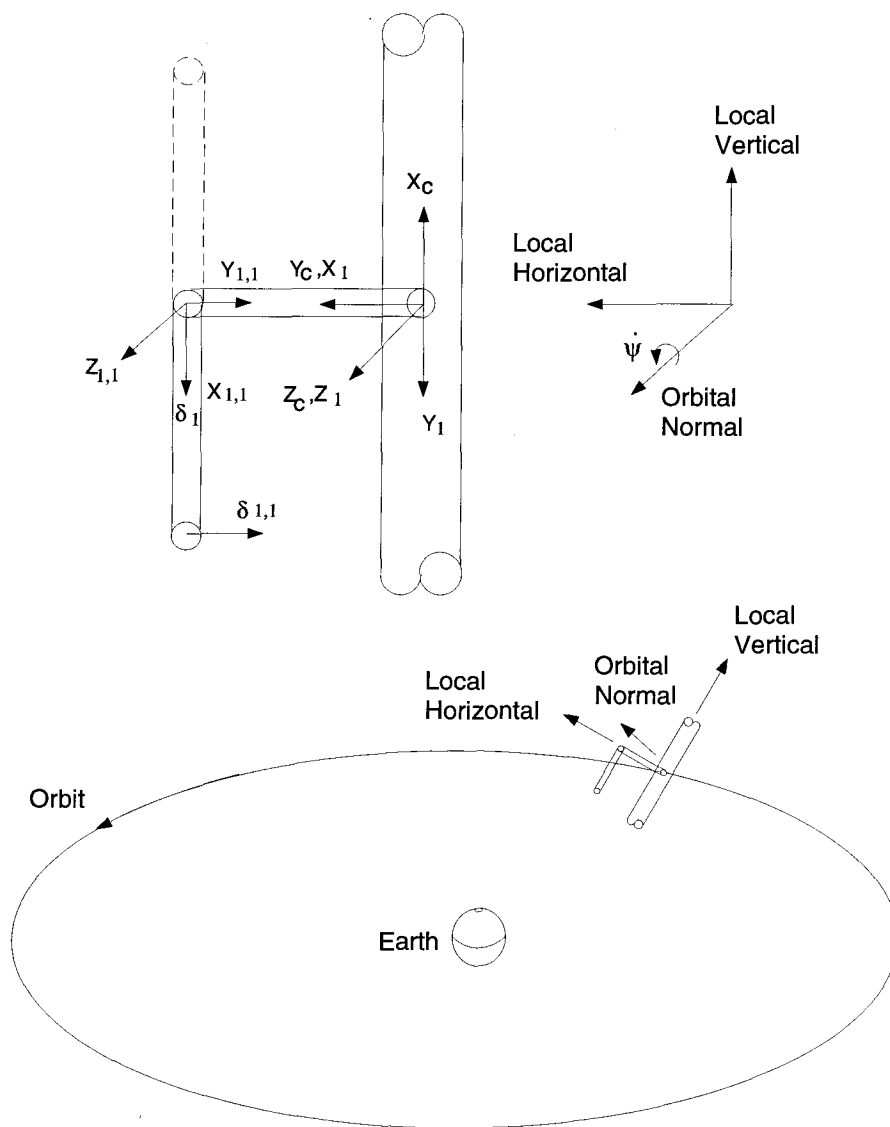


Figure 6.14: Geometry of the two-link manipulator supported by a rigid space platform.

i.e. the out-of plane librations, roll and yaw, remain zero. The response follows the expected trend. With the increase in amplitude and speed of the maneuver, from  $45^\circ$  at  $4.5^\circ/min$  to  $180^\circ$  at  $18^\circ/min$ , the peak pitch response increases from  $0.01^\circ$  to  $0.035^\circ$ . Corresponding vibratory response at the tip of the lower arm ( $\delta_{11}$ ) in the  $Y_{1,1}$  direction is also shown for the three cases. Note., the maximum  $\delta_{11}$  increases significantly, from 0.3mm to 1.2mm .

The effect of speed is isolated in the response results given in Figure (6.16). Now, the fixed inplane maneuver of  $180^\circ$  is completed at increasingly faster rates ( $18^\circ/min$ ,  $36^\circ/min$ , and  $90^\circ/min$ ). As can be expected, the librational response is modulated at the vibrational frequency with the pick  $\psi$  exceeding  $0.05^\circ$ . Note, the tip response at the lower arm exceeds 10cm for fastest maneuver considered ! This clearly suggests that active control would be necessary during large , fast maneuvers to maintain the response within an acceptable level.

Figure (6.17) assesses the effect of manipulator location on the system response for a  $180^\circ$  maneuver completed in 10 minutes. Two cases are considered : (a) manipulator located at the center of the station as before (same as Case (a) in Figure (6.16)); (b) manipulator located near the tip of the station. Note, besides the librational and manipulator tip response, deflection time history of the upper arm end ( $\delta_1$ ) is also plotted. As can be expected, several observations of interest can be made:

- (i) As expected, the pitch amplitude increases significantly due to a large reaction moment about the center of mass. In the present case it increases almost by a factor of 10 !
- (ii) The inplane deflection  $\delta_1$  of the upper arm is large than that of the lower arm  $\delta_{11}$ .
- (iii) Effect of the MSS location on the vibratory response of its arms, though present, is relatively small.

Figure (6.18) studies the effect MSS location during a faster maneuver of  $180^\circ$  in 5 minutes (twice the previous slewing rate). Except for the frequency modulation in the pitch, the response character remains essentially the same as in Figure (6.17).

Next the attention was turned to the system response with the librational control using the FLT. Typical results are given for the influence of the slewing speed with the manipulator located at the center of the system in Figures (6.19)-(6.21) and at the tip of the station Figures (6.22)-(6.23). Note, the librational motion is controlled, as expected, quite well depending upon the choice of gains. The vibratory motion being uncontrolled continues to persist as no damping is considered. There are several options available to control the manipulator vibrations using the conventional proportional control strategies, linear or nonlinear, with or without damping. These options are not pursued here as the main objective is to assess applicability of the FLT to this class of system. The extension to a hybrid control strategy with the FLT applied to the librational degrees and proportional (or other conventional control) control procedure applied to the vibrational degrees is rather routine.

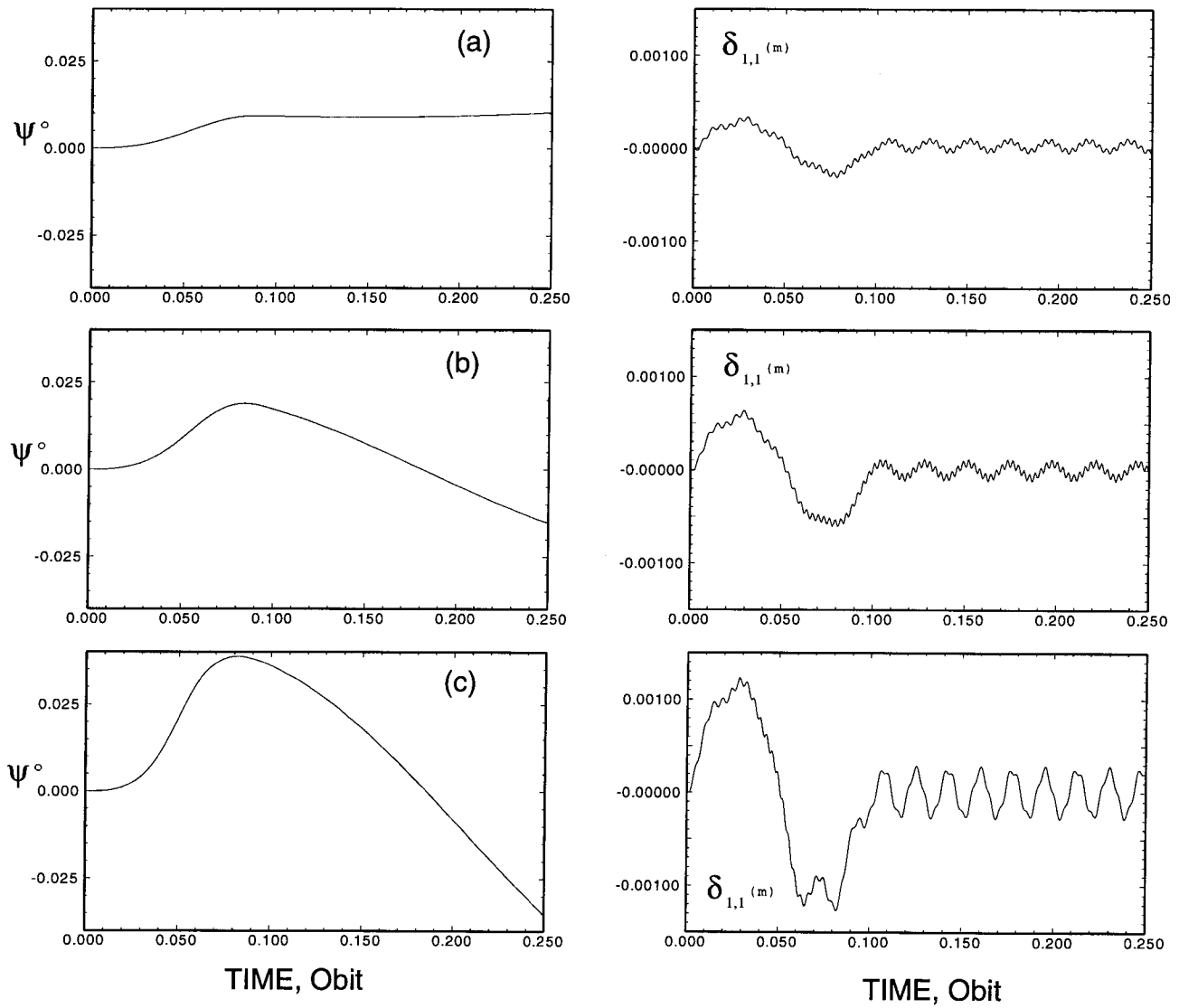


Figure 6.15: Effect of increasing the amplitude as well as speed of the slewing maneuver, in the plane of the orbit, with the MSS located at the center of the station: (a)  $45^\circ$  in 10 min; (b)  $90^\circ$  in 10 min; (c)  $180^\circ$  in 10 min.

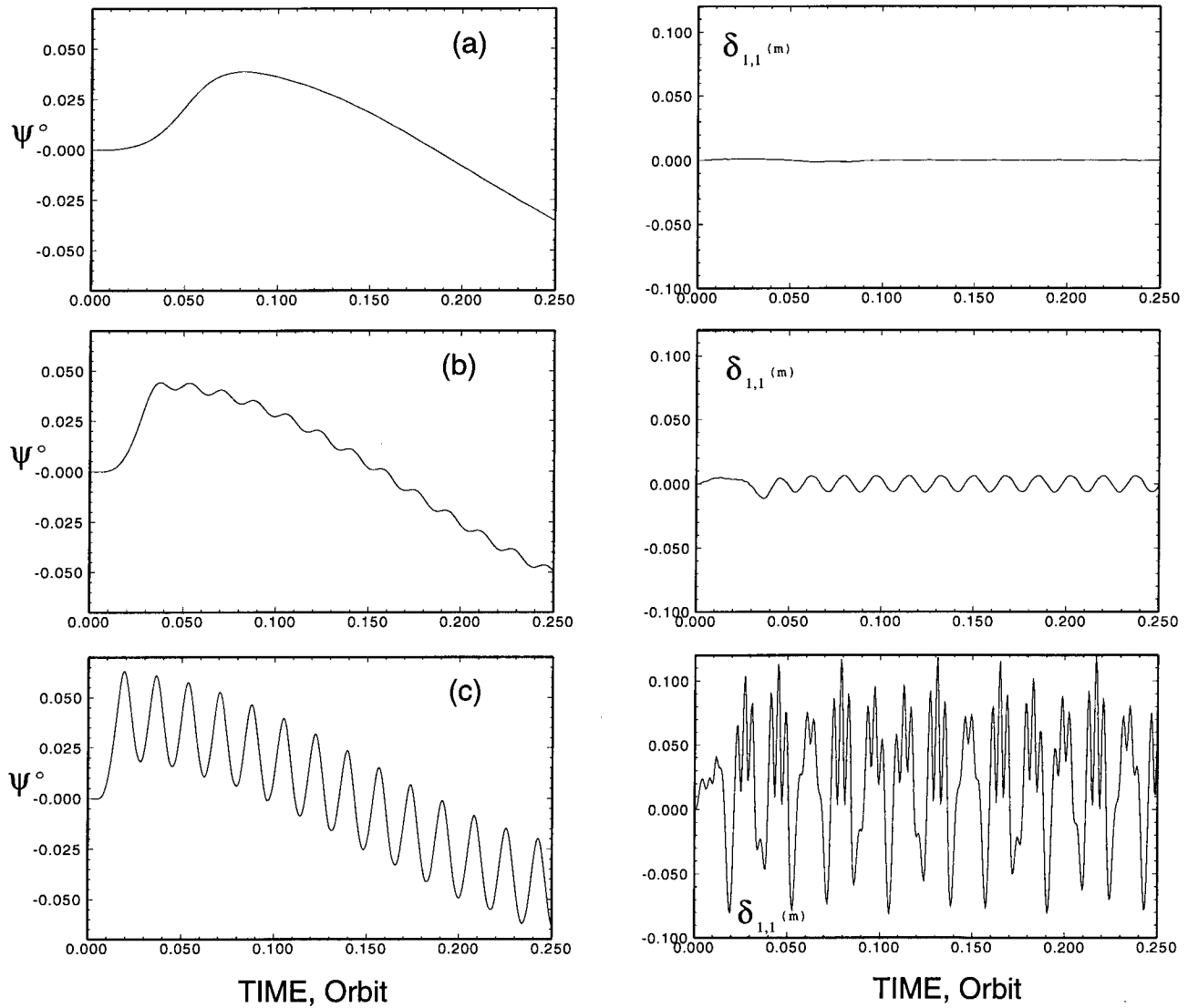


Figure 6.16: Effect of the slewing speed on the system response with the manipulator at the center of the main truss. The slewing maneuver of  $180^\circ$  (inplane) is completed in: (a) 10 min; (b) 5 min; (c) 2 min.

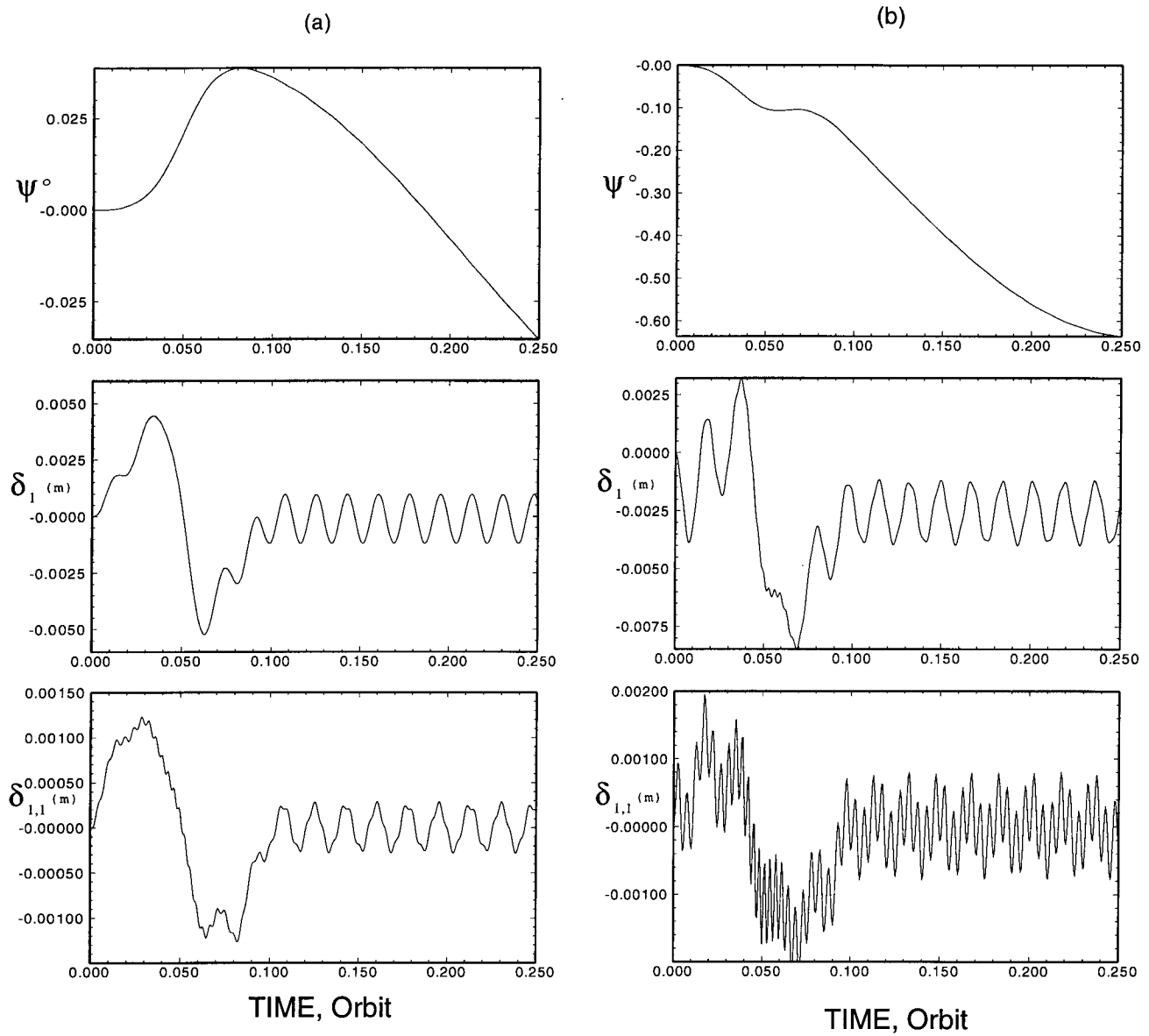


Figure 6.17: Response plots showing the effect of the manipulator's location: (a) Manipulator at the center of the station; (b) manipulator at the tip of the station. The slewing rate is  $180^\circ$  in 10 min.

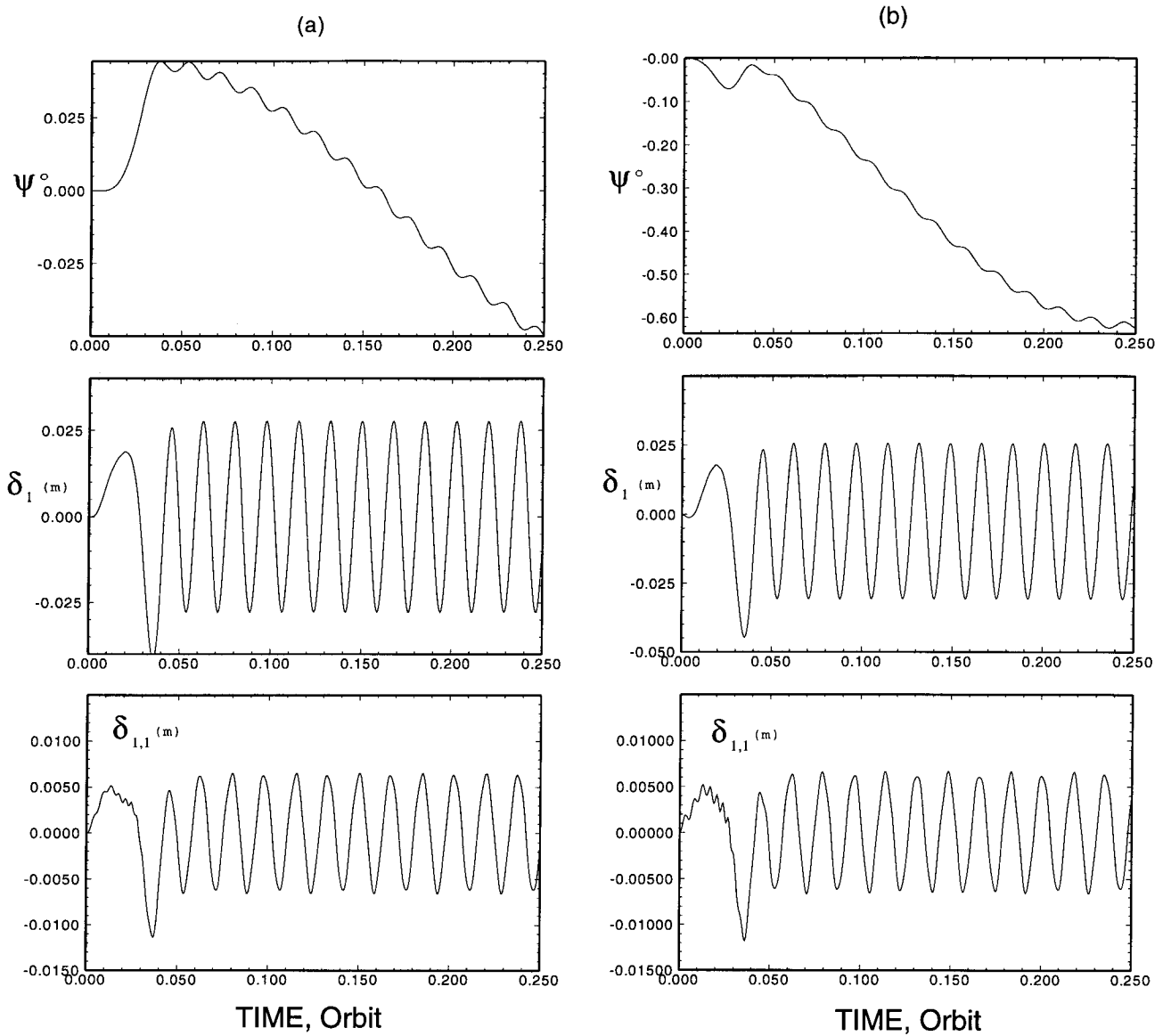


Figure 6.18: Response plots showing the effect of the manipulator's location during the slewing maneuver of  $180^\circ$  in 5 min. (a) manipulator at the center of the station (b) manipulator at the tip of the station.

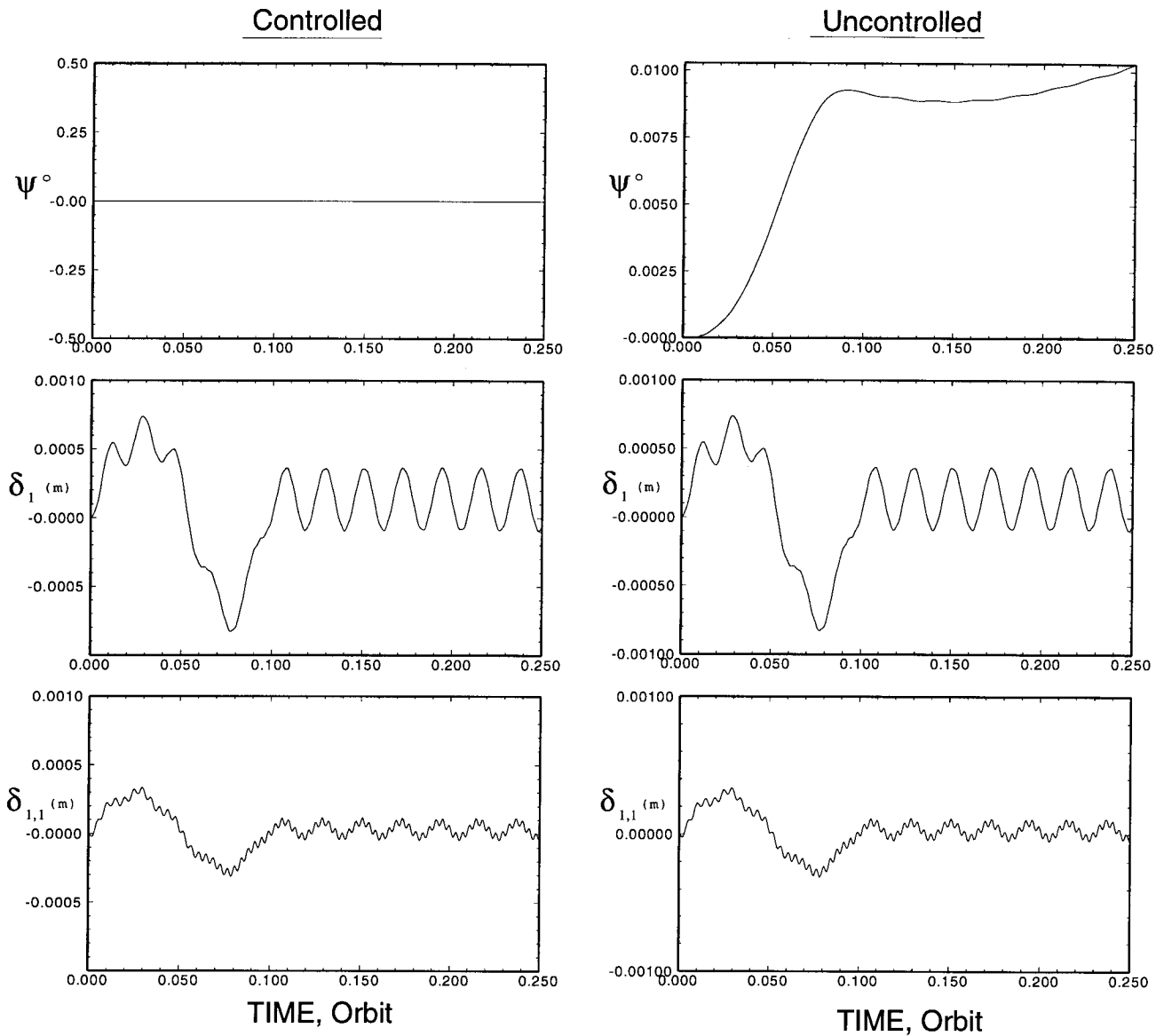


Figure 6.19: Controlled response using the FLT applied to the librational degrees of freedom with the manipulator at the center of the station: slewing maneuver of  $45^\circ$  in 10 minutes.

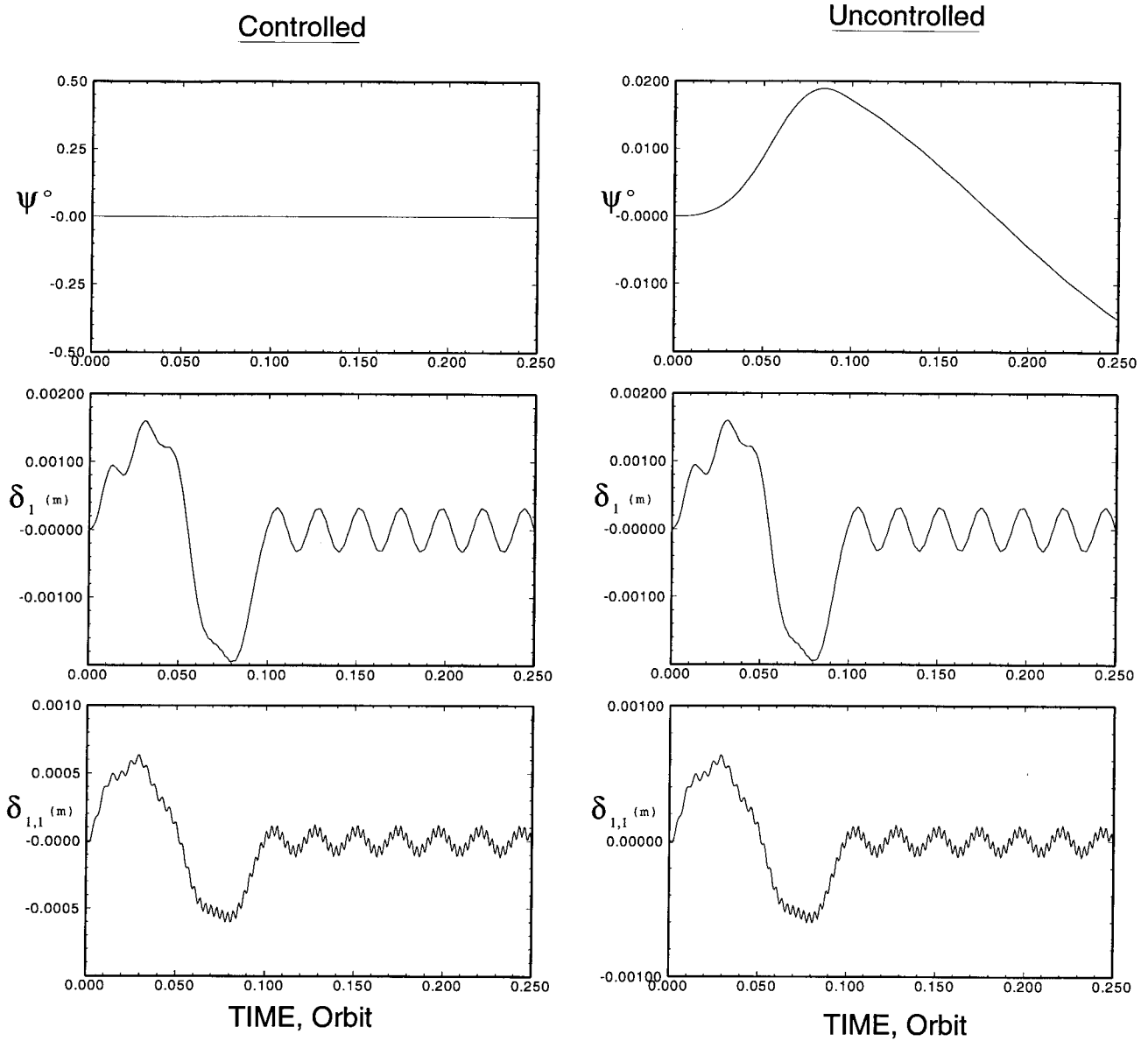


Figure 6.20: Controlled response using the FLT applied to the librational degrees of freedom with the manipulator at the center of the station: slewing maneuver of  $90^\circ$  in 10 minutes.

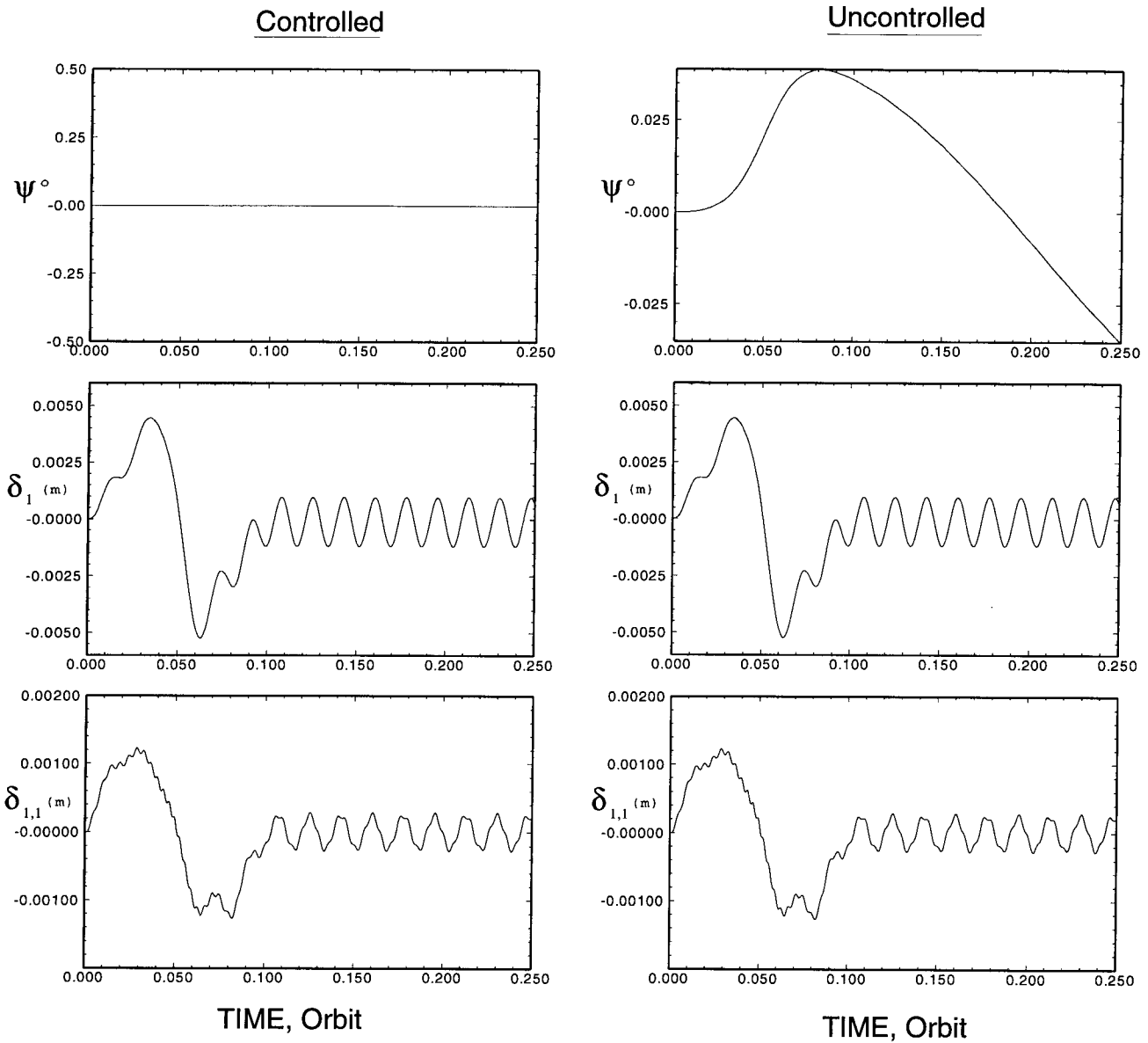


Figure 6.21: Controlled response using the FLT applied to the librational degrees of freedom with the manipulator at the center of the station: slewing maneuver of  $180^\circ$  in 10 minutes.

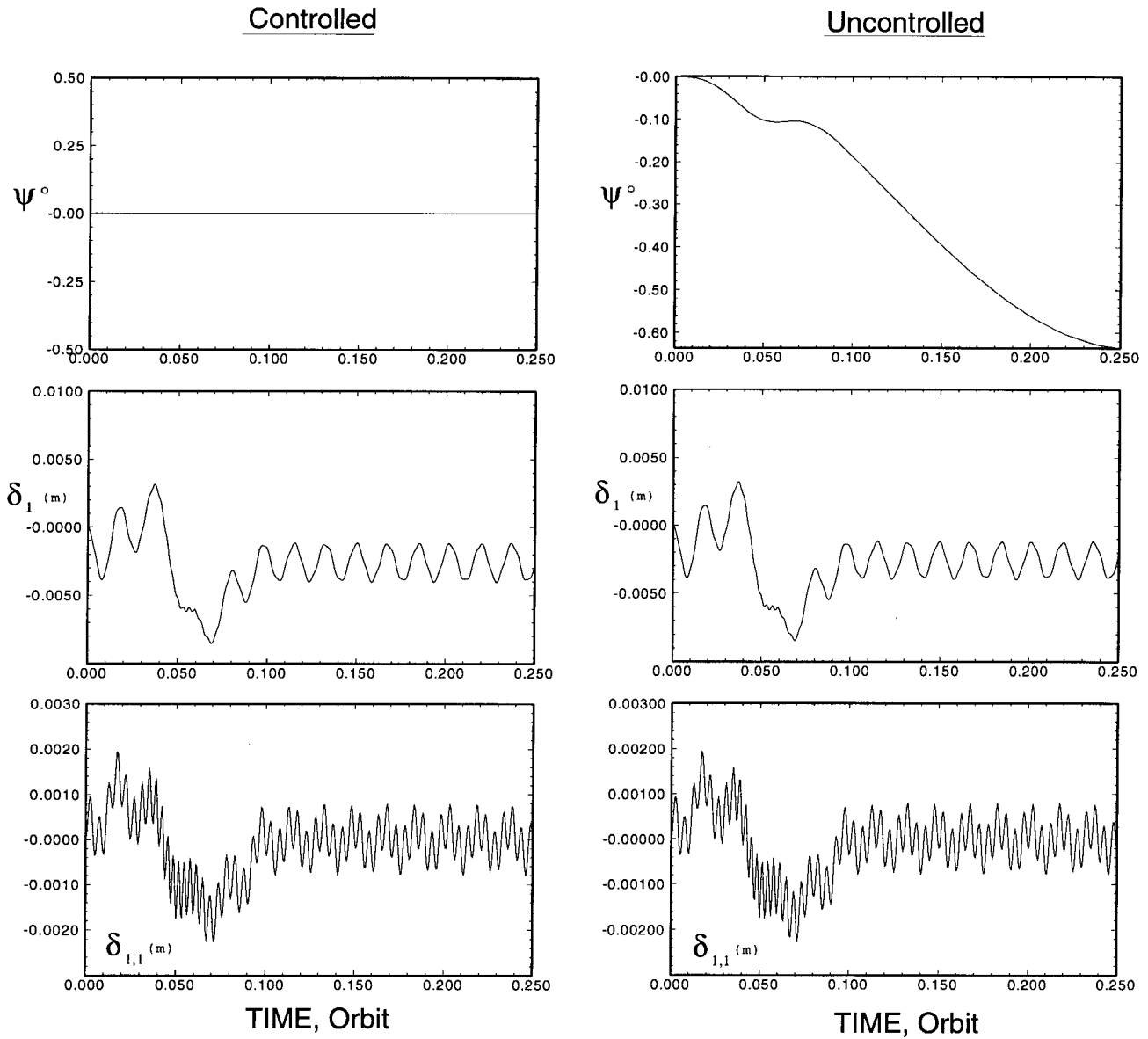


Figure 6.22: System response in the presence of FLT control with the manipulator located at the tip of the station: slewing maneuver of  $180^\circ$  in 10 minutes.

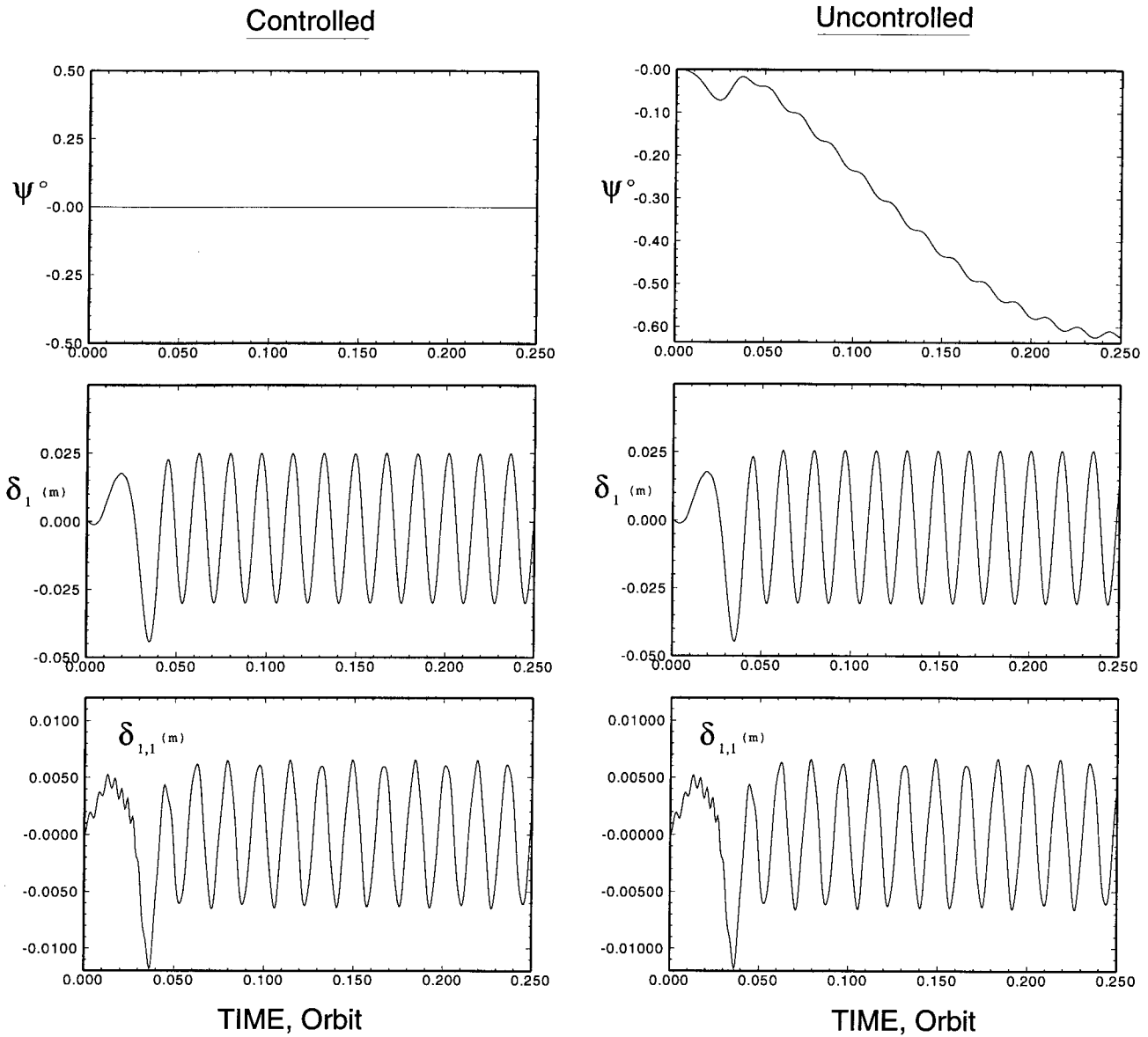


Figure 6.23: System response in the presence of FLT control with the manipulator located at the tip of the station: slewing maneuver of  $180^\circ$  in 5 minutes.

## 6.2 NASA's Control-Structure Interaction Model

As pointed out before, with increase in size of the space structures, flexibility effects have progressively become more important in ensuring successful completion of a given mission. The frequency spectrum for a flexible space based system often shows extremely low fundamental frequency with closely spaced and/or overlapping higher modes. This raises the possibility of the control system bandwidth interfering with the system dynamics making understanding of the Control-Structure-Interaction(CSI) problems and their resolution extremely important. This has led to the establishment of a major project by NASA, involving ground as well as space based experiments, to better appreciate the CSI oriented issues [9]. The CSI project has established an evolutionary structural model for dynamics and control study as shown in Figure (6.24). It consists of a uniform beam supporting a one arm flexible manipulator and a fixed rigid antenna. The manipulator can be located at any desired position on the beam. Two such positions are shown in the figure: manipulator located at the center or the tip of the beam. Objective is to control the manipulator's tip position during slewing maneuvers. In the present study, this is attempted using the FLT with the flexibility discretization accomplished using system as well as component modes. Thus the response results would help assess:

- (i) effectiveness of the control strategy using the FLT;
- (ii) comparative response using the two discretization procedures.

The numerical values used in the simulation are presented in Table (6.2)

The manipulator, initially aligned with the main truss, executes a slewing maneuver of  $108^\circ$  in 10 minutes when located at: (i) the midpoint of the space station (beam); (ii) the tip of the truss, i.e. 57.5 m from the center. Corresponding results are given in Figures (6.25) and (6.26), respectively.

Table 6.2: Numerical values used during simulation of the CSI configuration dynamics

	M (kg)	L (m)	f(Hz)	$I_{xx}$ (kgm <sup>2</sup> )	$I_{yy}$ (kgm <sup>2</sup> )	$I_{zz}$ (kgm <sup>2</sup> )
Main truss	18,000	115	0.193	$1.9733 \times 10^7$	$1.01 \times 10^4$	$1.9733 \times 10^7$
Link	3,200	15	0.015	1,805	25.500	25.500
Tip Point Mass	1,000	-	-	-	-	-

The results shows that the nonlinear control using the FLT continues to be quite effective. Both the manipulator and the truss tip motions are rather small. Furthermore, the general trend of the response time history is essentially the same except for local details. The main difference seems to be the chattering response with the SMM which is attributed to the updating of the system mode (fundamental) during the slewing maneuver. In the present case the new system mode was calculated every 2.78 minutes (100 min./36 steps), to save the computational effort. Of course, by more frequent updating, the chattering can be eliminated.

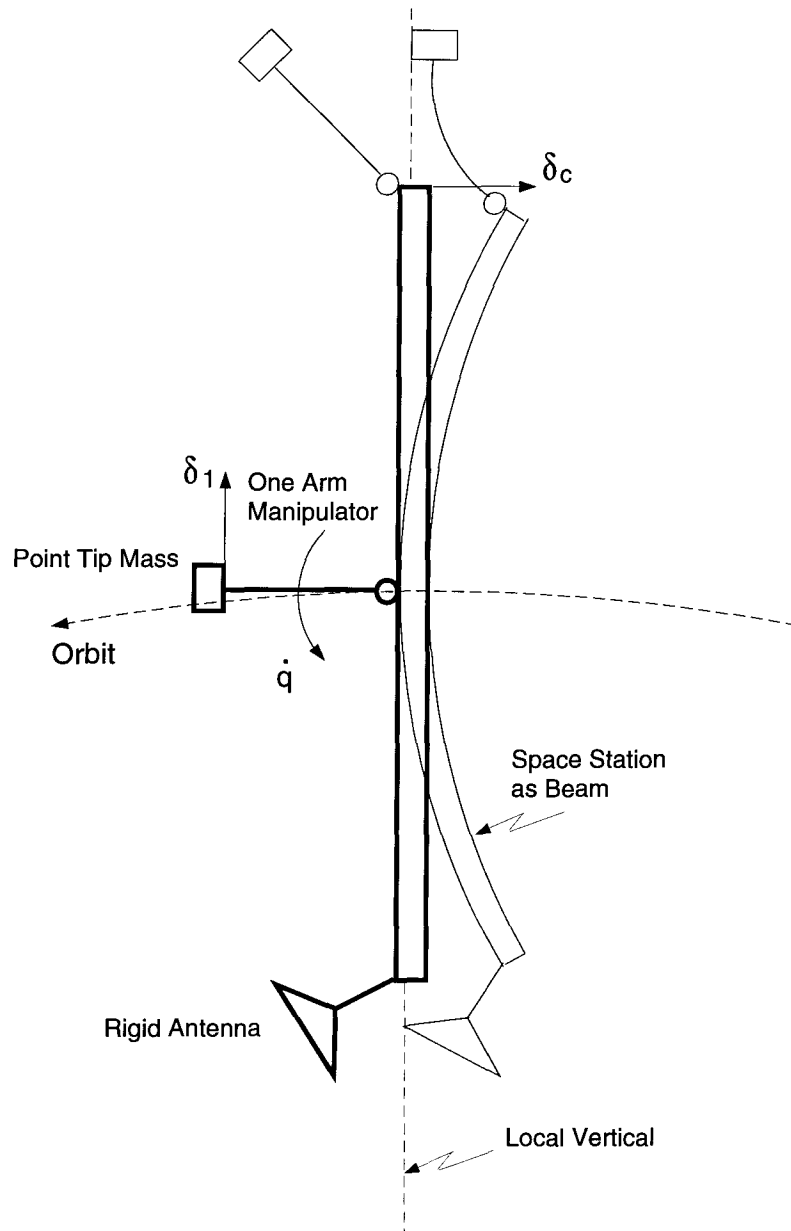


Figure 6.24: Geometry of the model proposed by NASA for the Control-Structure-Interaction (CSI) study.

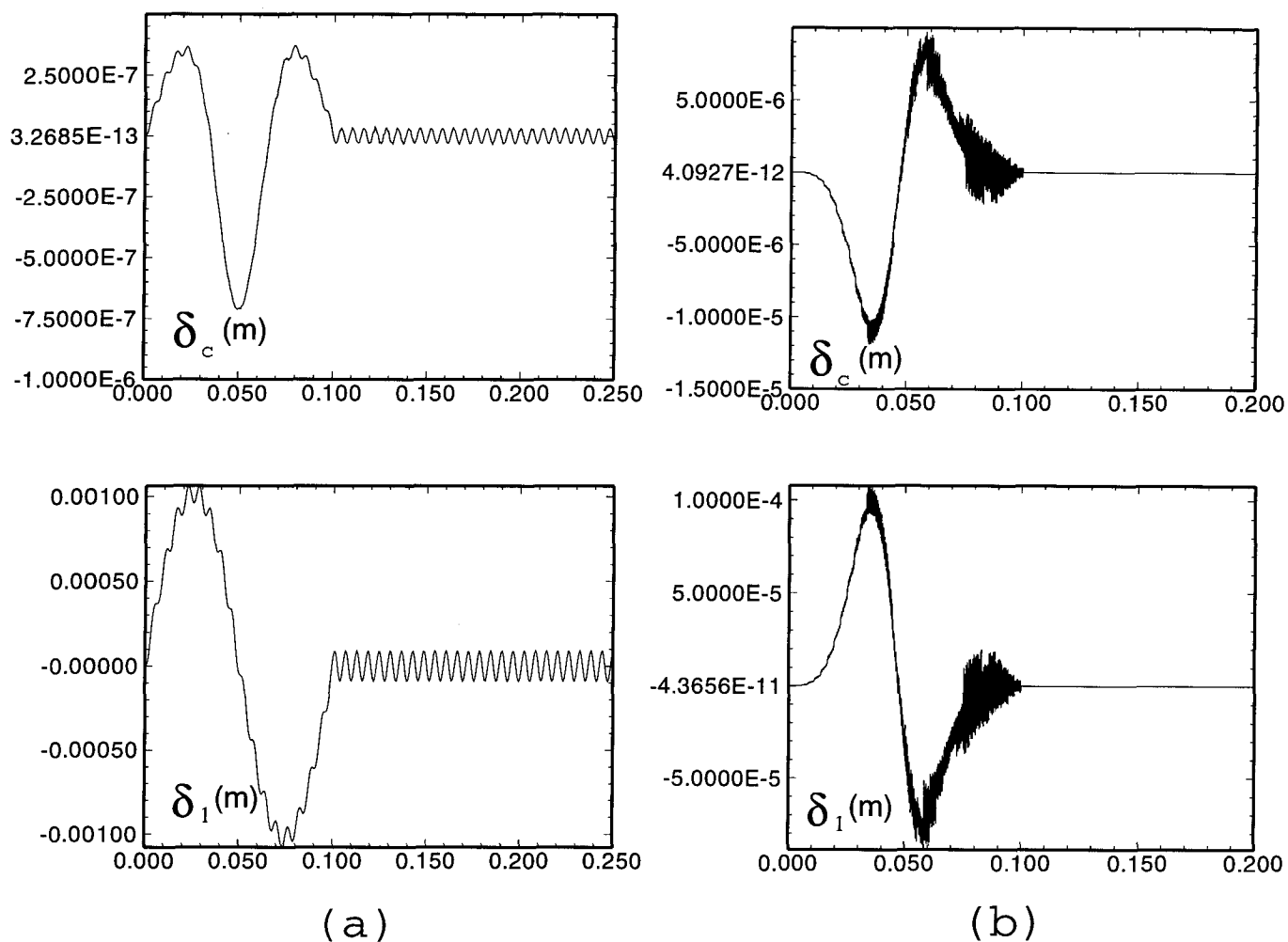


Figure 6.25: Response of the NASA's CSI model during a 180° maneuver in 10 minutes: (a) discretization using the CMM; (b) discretization using the SMM. The manipulator is located at the center of the truss.

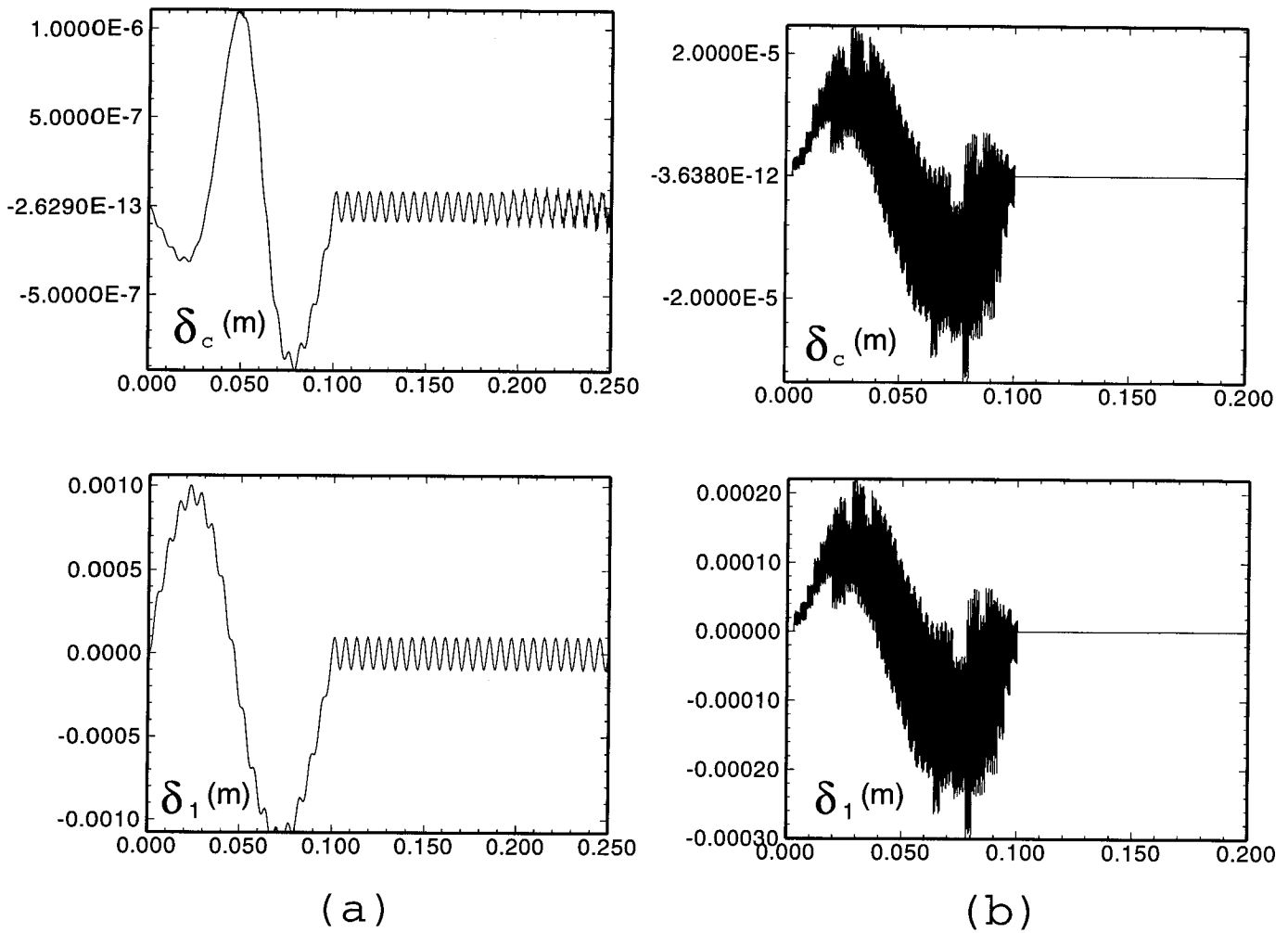


Figure 6.26: Effect of the manipulator location on the system response during the 180° slewing maneuver in 10 minutes: (a) discretization using the CMM; (b) discretization using the SMM. The manipulator is situated at the tip of the truss.

## Chapter 7

### CONCLUDING REMARKS AND RECOMMENDATIONS FOR FUTURE WORK

Advent of the computer revolution has made it possible for dynamicists and control engineers to analyze complex space based systems. Dynamics of a flexible orbiting platform, supporting a mobile flexible manipulator, represents a system never envisaged by pioneers of the classical mechanics including Newton, Euler, Lagrange and Hamilton. Yet, their elegant methodologies help us cast such formidable systems into mathematical models, and computers assist in their analyses.

The present thesis has attempted to tackle a class of such challenging problems of considerable practical importance. More important aspects of the study and associated results may be summarized as follows:

- (i) An approach to a relatively general formulation for studying dynamics and control of systems, characterized by interconnected flexible bodies, has been explained.
- (ii) A computer code for the above model, leading to extremely lengthy, highly nonlinear, nonautonomous and coupled equations of motion, has been developed.
- (iii) The formulation together with the operational integration program represent powerful tools for design and parametric evaluation of the system performance.
- (iv) Application of the above mentioned development to a specific system of the space station based flexible manipulator, in the presence of nonlinear FLT control, suggests versatility of the computer code. Results show that large and rapid maneuvers

can lead to unacceptable response. The information is fundamental to the design of the system as well as the controller.

- (v) The study using the NASA's control-structure interaction model shows the response trends to be essentially the same with the component or the system mode discretization. The differences are primarily local in character, at least for the case considered.

The study presents a first step in approaching even the preliminary level of understanding for the dynamics and control of complex flexible systems. The thesis has established a methodology, however, systematic parametric studies are necessary with a variety of configurations, of practical importance, to develop a data bank with performance and design charts. This would demand considerable time, effort and computer cost, but should lead to important design tools so urgently needed for the next generation of spacecraft. It will also help in planning of the proposed space based experiments aimed at dynamics and control of flexible structures, analysis of results when such experiments are conducted, with the assessment and improvement of the models and control algorithms.

## Bibliography

- [1] Modi, V.J., and Brereton, R.C., "Planar Librational Stability of a Flexible Satellites", *AIAA Journal*, Vol.6, No.3, March 1968, pp.511-517.
- [2] Modi, V.J., and Flanagan, R.C., "Effect of Environmental Forces on the Attitude Dynamics of Gravity Oriented Satellites, Part I: High Attitude Orbits", *The Aeronautical Journal of the Royal Aeronautical Society*, Vol.75, November 1971, pp.783-793.
- [3] Modi, V.J., and Flanagan, R.C., "Effect of Environmental Forces on the Attitude Dynamics of Gravity Oriented Satellites, Part II: Intermediate Altitude Orbits Accounting for Earth Radiation", *The Aeronautical Journal of the Royal Aeronautical Society*, Vol.75, December 1971, pp.846-849.
- [4] Flanagan, R.C., and Modi, V.J., "Effect of Environmental Forces on the Attitude Dynamics of Gravity Oriented Satellites, Part III: Close Earth Orbits Accounting for Aerodynamic Forces", *The Aeronautical Journal of the Royal Aeronautical Society*, Vol.76, January 1972, pp.34-40.
- [5] Modi, V.J., and Flanagan, R.C., "Librational Damping of a Gravity Oriented System Using Solar Radiation Pressure", *The Aeronautical Journal of the Royal Aeronautical Society*, Vol.75, August 1971, pp.560-564.
- [6] Modi, V.J., and Kumar, K., "Librational Dynamics of a Satellite with Thermally Flexed Appendages", *The Journal of the Astronautical Sciences*, Vol.25, No.1, January-March 1977, pp.3-20.
- [7] Ibrahim, A.M., *Mathematical Modelling of Flexible Multibody Dynamics with Applications to Orbiting Systems*, Ph.D. Thesis, The University of British Columbia, April 1988.
- [8] Chan, J.K., *Dynamics and Control of an Orbiting Space Platform Based Mobile Flexible Manipulator*, M.A.Sc. Thesis, The University of British Columbia, Vancouver, Canada, April 1990.
- [9] Special Issue on Computer Methods in Flexible Multibody Dynamics, *The International Journal of Numerical Methods in Engineering*, Vol.32, No.8, December 1991.
- [10] Modi, V.J., "Attitude Dynamics of Satellites with Flexible Appendages- A Brief Review", *Journal of Spacecraft and Rocket*, Vol.58, No. 11, November 1974, pp.743-751.

- [11] Modi,V.J., "Spacecraft attitude Dynamics : Evolution and Current Challenges", Invited Address to the *NATO/AGARD Symposium on the Space Vehicle Flight Mechanics*, Luxembourg, November 1989; also *Proceedings of the Symposium*, AGARD-CP-489, pp.15-1 to 15-26; also *Acta Astronautica*, Vol.21 No.10, 1990, pp.689-718.
- [12] Ng,A.C., *Dynamics and Control of Orbiting Flexible Systems:A Formulation with Applications*, Ph.D.Thesis, The University of British Columbia, Vancouver, Canada, April 1992.
- [13] Suleman,A., *Dynamics and Control of Evolving Space Platforms: an Approach with Application*, Ph.D. Thesis, The University of British Columbia, Vancouver,Canada, August 1992.
- [14] Mah,H.W., *On the Nonlinear Dynamics of a Space Platform Based Mobile Flexible Manipulator*, Ph.D. Thesis, The University of British Columbia, Vancouver, Canada. October 1992.
- [15] NASA Langley Material on the Space Station *Freedom* as a Transportation Node and the NASA CSI Program, NASA Langley Space Station Office and CSI Program Office.
- [16] Mah, H.W., and Modi, V.J., " A Relatively General Formulation for Studying Dynamics of the Space Station Based MRMS with Applications", *AIAA 26th Aerospace Sciences Meeting*, January 1988 Reno,Nevada,U.S.A., paper No.AIAA-88-0674.
- [17] Modi, V.J.,and Suleman,A., " An Approach to Dynamics of Flexible Orbiting Systems with Application to the Proposed Space Station", *42nd Congress of the International Astronautical Federation*, October 1991, Montreal, Canada , Paper No.IAF-91-293.
- [18] Ng, A.C, and Modi, V.J., " Dynamics of Gravity Oriented satellites with Thermally Flexed Appendages", *AAS/AIAA Astrodynamics Specialist Conference, Kalispell, Montana,U.S.A.*, 1987, Paper No. AAS-87-432.
- [19] Misawa, E.A., and Hedrick, J.K., " Nonlinear Observers-A State-of -the-Art Survey", *ASME Journal of Dynamic Systems, Measurement, and Control*, Vol.111, September 1989, pp.344-352.
- [20] Baumann, W.T., and Rugh, W.J., " Feedback Control of Nonlinear Systems By Extended Linearization", *IEEE Journal of Automatic Control*, Vol.31, No.1, January 1986, pp.40-46.

- [21] Baumann, W.T., "Feedback Control of Multi-input Nonlinear Systems by Extended Linearization", *IEEE Journal of Automatic Control*, Vol.33, No.2, February 1988, pp.193-197.
- [22] Wang, D., and Vidyasagar, M., "Control of a Class of Manipulators with a Single Flexible Link-Part I: Feedback Linearization", *ASME Journal of Dynamic Systems, Measurement, and Control*, Vol.11, December 1991, pp.655-661.
- [23] Wang, D., and Vidyasagar, M., "Control of a Class of Manipulators with a Single Flexible Link-Part II: Observer-Controller Stabilization", *ASME Journal of Dynamic Systems, Measurement, and Control*, Vol. 11, December 1991, pp.662-668.
- [24] Modi, V.J., Karray, F., and Chan, J.K., "On the Control of a Class of Flexible Manipulators Using Feedback Linearization Approach", *42nd Congress of the International Astronautical Federation*, October 1991, Montreal, Canada, Paper No. IAF-91-324.
- [25] Karray, F., Modi, V.J., and Chan, J.K., "Inverse Control of Flexible Orbiting Manipulators", *Proceedings of the American Control Conference*, Boston, Mass. U.S.A., June 1991, Editor: A.G. Ulsoy, pp. 1909-1912.
- [26] Sharan, A.M., Jain, J., and Kalra, P., "Efficient Methods for Solving Dynamic Problems of Flexible Manipulators", *ASME Journal of Dynamic Systems, Measurement, and Control*, Vol.114, March 1992, pp.78-88.
- [27] Tosunoglu, S., Lin, S.H., and Tesar, D., "Accessibility and Controllability of Flexible Robotic Manipulators", *ASME Journal of Dynamic Systems, Measurement, and Control*, Vol.114, March 1992, pp.50-58.
- [28] Fuliu, V., Rattan, K.S, and Brown Jr., H.B., "Modeling and Control of Single-Link Flexible Arms with Lumped Masses", *ASME Journal of Dynamic Systems, Measurement, and Control*, Vol.114, March 1992, pp.59-69.
- [29] Spong, M.W., and Vidyasagar, M., "Robust Linear Compensator Design for Nonlinear Robotic Control", *Proceedings of the IEEE Conference on Robotics and Automation*, St. Louis, Missouri, U.S.A., March 1985, pp.954-959.
- [30] Spong, M.W., and Vidyasagar, M., "Robust Nonlinear Control of Robot Manipulator", *Proceedings of the 24th IEEE Conference on Decision and Control*, Fort Lauderdale, Florida, U.S.A., December 1985, pp. 1767-1772.
- [31] De Silva, C.W., "Trajectory Design for Robotic Manipulator in Space Application", *J.Guidance, Control and Dynamics*, Vol.14, No.3, 1991, pp.670-674.

- [32] Xu, J., Bainum, P.M., and Li, F., "Reaction Rejection Techniques for Control of Space-Robotic Structures", *IMACS/SICE International Symposium on Robotics, Mechatronics and Manufacturing Systems*, Kobe, Japan, September 1992.

## Appendix A

### DETAILS OF $T_{sys}$ , $I_{sys}$ AND $\bar{H}_{sys}$

The details of the components that make up  $T$  of Eq.(3.31) are as follows:

$$T_{orb} = \frac{1}{2} M \dot{\bar{R}}_{cm} \cdot \dot{\bar{R}}_{cm};$$

$$T_{cm} = -\frac{1}{2} M \dot{\bar{C}}_{cm} \cdot \dot{\bar{C}}_{cm};$$

$$T_h = \frac{1}{2} \sum_{i=1}^N \left[ \int_{m_i} \dot{\bar{d}} \cdot \dot{\bar{d}} dm_i + \sum_{j=1}^{n_i} \int_{m_{i,j}} (\dot{\bar{d}}_i + C_i^c \dot{\bar{d}}_{ij}) \cdot (\dot{\bar{d}}_i + C_i^c \dot{\bar{d}}_{ij}) dm_{i,j} \right];$$

$$\begin{aligned} T_{jr} = & \frac{1}{2} \sum_{i=1}^N \left[ \int_{m_i} \dot{C}_i^c (\bar{\rho}_i + \bar{\tau}_i + \bar{\delta}_i) \cdot \dot{C}_i^c (\bar{\rho}_i + \bar{\tau}_i + \bar{\delta}_i) dm_i \right. \\ & + \sum_{j=1}^{n_i} \int_{m_{i,j}} \left\{ \dot{C}_i^c \bar{d}_{ij} + (\dot{C}_{i,j}^c \mu_{i,j} + C_{i,j}^c \dot{\mu}_{i,j}) (\bar{\rho}_{ij} + \bar{\tau}_{ij} + \bar{\delta}_{ij}) \right\} \cdot \\ & \left. \left\{ \dot{C}_i^c \bar{d}_{ij} + (\dot{C}_{i,j}^c \mu_{i,j} + C_{i,j}^c \dot{\mu}_{i,j}) (\bar{\rho}_{ij} + \bar{\tau}_{ij} + \bar{\delta}_{ij}) \right\} dm_{i,j} \right]; \end{aligned}$$

$$T_t = \frac{1}{2} \int_{m_c} \dot{\bar{\tau}}_c \cdot \dot{\bar{\tau}}_c dm_c + \frac{1}{2} \sum_{i=1}^N \left[ \int_{m_i} (C_i^c \dot{\bar{\tau}}_i) \cdot (C_i^c \dot{\bar{\tau}}_i) dm_i \right]$$

$$+ \sum_{j=1}^{n_i} \int_{m_{i,j}} (C_{i,j}^c \mu_{i,j} \dot{\bar{\tau}}_{ij}) \cdot (C_{i,j}^c \mu_{i,j} \dot{\bar{\tau}}_{ij}) dm_{i,j} \Big];$$

$$T_v = \frac{1}{2} \int_{m_c} \dot{\bar{\delta}}_c \cdot \dot{\bar{\delta}}_c dm_c + \frac{1}{2} \sum_{i=1}^N \left[ \int_{m_i} (C_i^c \dot{\bar{\delta}}_i) \cdot (C_i^c \dot{\bar{\delta}}_i) dm_i \right. \\ \left. + \sum_{j=1}^{n_i} \int_{m_{i,j}} (C_{i,j}^c \mu_{i,j} \dot{\bar{\delta}}_{ij}) \cdot (C_{i,j}^c \mu_{i,j} \dot{\bar{\delta}}_{ij}) dm_{i,j} \right];$$

$$T_{h,jr} = \sum_{i=1}^N \left[ \int_{m_i} \dot{\bar{d}}_i \cdot \dot{C}_i^c (\bar{\rho}_i + \bar{\tau}_i + \bar{\delta}_i) dm_i + \sum_{j=1}^{n_i} \int_{m_{i,j}} \{ \dot{\bar{d}}_i + C_i^c \dot{\bar{d}}_{ij} \} \cdot \{ \dot{C}_i^c \bar{d}_{ij} + (\dot{C}_{i,j}^c \mu_{i,j} + C_{i,j}^c \dot{\mu}_{i,j}) (\bar{\rho}_{ij} + \bar{\tau}_{ij} + \bar{\delta}_{ij}) \} dm_{i,j} \right];$$

$$T_{h,t} = \sum_{i=1}^N \left[ \int_{m_i} \dot{\bar{d}}_i \cdot (\dot{C}_i^c \dot{\bar{\tau}}_i) dm_i + \sum_{j=1}^{n_i} \int_{m_{i,j}} (\dot{\bar{d}}_i + C_i^c \dot{\bar{d}}_{ij}) \cdot (C_{i,j}^c \mu_{i,j} \dot{\bar{\tau}}_{ij}) dm_{i,j} \right];$$

$$T_{h,v} = \sum_{i=1}^N \left[ \int_{m_i} \dot{\bar{d}}_i \cdot (C_i^c \dot{\bar{\delta}}_i) dm_i + \sum_{j=1}^{n_i} \int_{m_{i,j}} (\dot{\bar{d}}_i + C_i^c \dot{\bar{d}}_{ij}) \cdot (C_{i,j}^c \mu_{i,j} \dot{\bar{\delta}}_{ij}) dm_{i,j} \right];$$

$$T_{jr,t} = \sum_{i=1}^N \left[ \int_{m_i} \dot{C}_i^c (\bar{\rho}_i + \bar{\tau}_i + \bar{\delta}_i) (\dot{C}_i^c \dot{\bar{\tau}}_i) dm_i + \sum_{j=1}^{n_i} \int_{m_{i,j}} \{ \dot{C}_i^c \bar{d}_{ij} + (\dot{C}_{i,j}^c \mu_{i,j} + C_{i,j}^c \dot{\mu}_{i,j}) (\bar{\rho}_{ij} + \bar{\tau}_{ij} + \bar{\delta}_{ij}) \} \cdot (C_{i,j}^c \mu_{i,j} \dot{\bar{\tau}}_{ij}) dm_{i,j} \right];$$

$$T_{jr,v} = \sum_{i=1}^N \left[ \int_{m_i} \dot{C}_i^c (\bar{\rho}_i + \bar{\tau}_i + \bar{\delta}_i) (\dot{C}_i^c \bar{\delta}_i) dm_i + \right. \\ \left. \sum_{j=1}^{n_i} \int_{m_{i,j}} \left\{ \dot{C}_i^c \bar{d}_{ij} + (\dot{C}_{i,j}^c \mu_{i,j} + C_{i,j}^c \dot{\mu}_{i,j}) (\bar{\rho}_{ij} + \bar{\tau}_{ij} + \bar{\delta}_{ij}) \right\} \right. \\ \left. \cdot (C_{i,j}^c \mu_{i,j} \dot{\bar{\delta}}_{ij}) dm_{i,j} \right];$$

$$T_{t,v} = \int_{m_c} \dot{\bar{\tau}}_c \cdot \dot{\bar{\delta}}_c dm_c + \sum_{i=1}^N \left[ \int_{m_i} (C_i^c \dot{\bar{\tau}}_i) \cdot (C_i^c \dot{\bar{\delta}}_i) dm_i \right. \\ \left. + \sum_{j=1}^{n_i} \int_{m_{i,j}} (C_{i,j}^c \mu_{i,j} \dot{\bar{\tau}}_{ij}) \cdot (C_{i,j}^c \mu_{i,j} \dot{\bar{\delta}}_{ij}) dm_{i,j} \right].$$

The system inertia,  $I_{sys}$ , given by Eq.(3.33) is the sum of the following components:

$$I_{cm} = -M \left[ \bar{C}_{cm} \cdot \bar{C}_{cm} U - \bar{C}_{cm} \bar{C}_{cm} \right];$$

$$I_h = \sum_{i=1}^N \left[ \int_{m_i} \{ \bar{d}_i \cdot \bar{d}_i U - \bar{d}_i \bar{d}_i \} dm_i + \sum_{j=1}^{n_i} \int_{m_{i,j}} \{ (\bar{d}_i + C_i^c \bar{d}_{i,j}) \cdot (\bar{d}_i + C_i^c \bar{d}_{i,j}) U \right. \\ \left. - (\bar{d}_i + C_i^c \bar{d}_{i,j}) (\bar{d}_i + C_i^c \bar{d}_{i,j}) \} dm_{i,j} \right];$$

$$I_r = \int_{m_c} \{ \bar{\rho}_c \cdot \bar{\rho}_c U - \bar{\rho}_c \bar{\rho}_c \} dm_c$$

$$\begin{aligned}
& + \sum_{i=1}^N \left[ \int_{m_i} \{ (C_i^c \bar{\rho}_i) \cdot (C_i^c \bar{\rho}_i) U - (C_i^c \bar{\rho}_i)(C_i^c \bar{\rho}_i) \} dm_i \right. \\
& + \sum_{j=1}^{n_i} \int_{m_{i,j}} \{ (C_{i,j}^c \mu_{i,j} \bar{\rho}_{ij}) \cdot (C_{i,j}^c \mu_{i,j} \bar{\rho}_{ij}) U \\
& \left. - (C_{i,j}^c \mu_{i,j} \bar{\rho}_{ij})(C_{i,j}^c \mu_{i,j} \bar{\rho}_{ij}) \} dm_{i,j} \right];
\end{aligned}$$

$$\begin{aligned}
I_t = & \int_{m_c} \{ \bar{\tau}_c \cdot \bar{\tau}_c U - \bar{\tau}_c \bar{\tau}_c \} dm_c \\
& + \sum_{i=1}^N \left[ \int_{m_i} \{ (C_i^c \bar{\tau}_i) \cdot (C_i^c \bar{\tau}_i) U - (C_i^c \bar{\tau}_i)(C_i^c \bar{\tau}_i) \} dm_i \right. \\
& + \sum_{j=1}^{n_i} \int_{m_{i,j}} \{ (C_{i,j}^c \mu_{i,j} \bar{\tau}_{ij}) \cdot (C_{i,j}^c \mu_{i,j} \bar{\tau}_{ij}) U \\
& \left. - (C_{i,j}^c \mu_{i,j} \bar{\tau}_{ij})(C_{i,j}^c \mu_{i,j} \bar{\tau}_{ij}) \} dm_{i,j} \right];
\end{aligned}$$

$$\begin{aligned}
I_v = & \int_{m_c} \{ \bar{\delta}_c \cdot \bar{\delta}_c U - \bar{\delta}_c \bar{\delta}_c \} dm_c \\
& + \sum_{i=1}^N \left[ \int_{m_i} \{ (C_i^c \bar{\delta}_i) \cdot (C_i^c \bar{\delta}_i) U - (C_i^c \bar{\delta}_i)(C_i^c \bar{\delta}_i) \} dm_i \right. \\
& + \sum_{j=1}^{n_i} \int_{m_{i,j}} \{ (C_{i,j}^c \mu_{i,j} \bar{\delta}_{ij}) \cdot (C_{i,j}^c \mu_{i,j} \bar{\delta}_{ij}) U \\
& \left. - (C_{i,j}^c \mu_{i,j} \bar{\delta}_{ij})(C_{i,j}^c \mu_{i,j} \bar{\delta}_{ij}) \} dm_{i,j} \right];
\end{aligned}$$

$$\begin{aligned}
I_{h,r} = & \sum_{i=1}^N \left[ \int_{m_i} \{2\bar{d}_i \cdot (C_i^c \bar{\rho}_i) U - \bar{d}_i (C_i^c \bar{\rho}_i) - (C_i^c \bar{\rho}_i) \bar{d}_i\} dm_i \right. \\
& + \sum_{j=1}^{n_i} \int_{m_{i,j}} \{2(\bar{d}_i + C_i^c \bar{d}_{ij}) \cdot (C_{i,j}^c \mu_{i,j} \bar{\rho}_{ij}) U - (\bar{d}_i + C_i^c \bar{d}_{ij})(C_{i,j}^c \mu_{i,j} \bar{\rho}_{ij}) \\
& \left. - (C_{i,j}^c \mu_{i,j} \bar{\rho}_{ij})(\bar{d}_i + C_i^c \bar{d}_{ij})\} dm_{i,j} \right];
\end{aligned}$$

$$\begin{aligned}
I_{h,t} = & \sum_{i=1}^N \left[ \int_{m_i} \{2\bar{d}_i \cdot (C_i^c \bar{\tau}_i) U - \bar{d}_i (C_i^c \bar{\tau}_i) - (C_i^c \bar{\tau}_i) \bar{d}_i\} dm_i \right. \\
& + \sum_{j=1}^{n_i} \int_{m_{i,j}} \{2(\bar{d}_i + C_i^c \bar{d}_{ij}) \cdot (C_{i,j}^c \mu_{i,j} \bar{\tau}_{ij}) U - (\bar{d}_i + C_i^c \bar{d}_{ij})(C_{i,j}^c \mu_{i,j} \bar{\tau}_{ij}) \\
& \left. - (C_{i,j}^c \mu_{i,j} \bar{\tau}_{ij})(\bar{d}_i + C_i^c \bar{d}_{ij})\} dm_{i,j} \right];
\end{aligned}$$

$$\begin{aligned}
I_{h,v} = & \sum_{i=1}^N \left[ \int_{m_i} \{2\bar{d}_i \cdot (C_i^c \bar{\delta}_i) U - \bar{d}_i (C_i^c \bar{\delta}_i) - (C_i^c \bar{\delta}_i) \bar{d}_i\} dm_i \right. \\
& + \sum_{j=1}^{n_i} \int_{m_{i,j}} \{2(\bar{d}_i + C_i^c \bar{d}_{ij}) \cdot (C_{i,j}^c \mu_{i,j} \bar{\delta}_{ij}) U - (\bar{d}_i + C_i^c \bar{d}_{ij})(C_{i,j}^c \mu_{i,j} \bar{\delta}_{ij}) \\
& \left. - (C_{i,j}^c \mu_{i,j} \bar{\delta}_{ij})(\bar{d}_i + C_i^c \bar{d}_{ij})\} dm_{i,j} \right];
\end{aligned}$$

$$\begin{aligned}
I_{\tau,t} = & \int_{m_c} \{2\bar{\rho}_c \cdot \bar{\tau}_c U - \bar{\rho}_c \bar{\tau}_c - \bar{\tau}_c \bar{\rho}_c\} dm_c \\
& + \sum_{i=1}^N \left[ \int_{m_i} \{2(C_i^c \bar{\rho}_i) \cdot (C_i^c \bar{\tau}_i) U - (C_i^c \bar{\rho}_i)(C_i^c \bar{\tau}_i) - (C_i^c \bar{\tau}_i)(C_i^c \bar{\rho}_i)\} dm_i \right.
\end{aligned}$$

$$\begin{aligned}
& + \sum_{j=1}^{n_i} \int_{m_{i,j}} \{2(C_{i,j}^c \mu_{i,j} \bar{\rho}_{ij}) \cdot (C_{i,j}^c \mu_{i,j} \bar{\tau}_{ij})U - (C_{i,j}^c \mu_{i,j} \bar{\rho}_{ij})(C_{i,j}^c \mu_{i,j} \bar{\tau}_{ij}) \\
& - (C_{i,j}^c \mu_{i,j} \bar{\tau}_{ij})(C_{i,j}^c \mu_{i,j} \bar{\rho}_{ij})\} dm_{i,j} ;
\end{aligned}$$

$$\begin{aligned}
I_{r,v} = & \int_{m_c} \{2\bar{\rho}_c \cdot \bar{\delta}_c U - \bar{\rho}_c \bar{\delta}_c - \bar{\delta}_c \bar{\rho}_c\} dm_c \\
& + \sum_{i=1}^N \left[ \int_{m_i} \{2(C_i^c \bar{\rho}_i) \cdot (C_i^c \bar{\delta}_i)U - (C_i^c \bar{\rho}_i)(C_i^c \bar{\delta}_i) - (C_i^c \bar{\delta}_i)(C_i^c \bar{\rho}_i)\} dm_i \right. \\
& + \sum_{j=1}^{n_i} \int_{m_{i,j}} \{2(C_{i,j}^c \mu_{i,j} \bar{\rho}_{ij}) \cdot (C_{i,j}^c \mu_{i,j} \bar{\delta}_{ij})U - (C_{i,j}^c \mu_{i,j} \bar{\rho}_{ij})(C_{i,j}^c \mu_{i,j} \bar{\delta}_{ij}) \\
& \left. - (C_{i,j}^c \mu_{i,j} \bar{\delta}_{ij})(C_{i,j}^c \mu_{i,j} \bar{\rho}_{ij})\} dm_{i,j} \right] ;
\end{aligned}$$

$$\begin{aligned}
I_{t,v} = & \int_{m_c} \{2\bar{\tau}_c \cdot \bar{\delta}_c U - \bar{\tau}_c \bar{\delta}_c - \bar{\delta}_c \bar{\tau}_c\} dm_c \\
& + \sum_{i=1}^N \left[ \int_{m_i} \{2(C_i^c \bar{\tau}_i) \cdot (C_i^c \bar{\delta}_i)U - (C_i^c \bar{\tau}_i)(C_i^c \bar{\delta}_i) - (C_i^c \bar{\delta}_i)(C_i^c \bar{\tau}_i)\} dm_i \right. \\
& + \sum_{j=1}^{n_i} \int_{m_{i,j}} \{2(C_{i,j}^c \mu_{i,j} \bar{\tau}_{ij}) \cdot (C_{i,j}^c \mu_{i,j} \bar{\delta}_{ij})U - (C_{i,j}^c \mu_{i,j} \bar{\tau}_{ij})(C_{i,j}^c \mu_{i,j} \bar{\delta}_{ij}) \\
& \left. - (C_{i,j}^c \mu_{i,j} \bar{\delta}_{ij})(C_{i,j}^c \mu_{i,j} \bar{\tau}_{ij})\} dm_{i,j} \right] .
\end{aligned}$$

Here,  $U$  is a unit matrix.

The components of  $\bar{H}_{sys}$ , the system angular momentum vector in Eq.(3.34) , are as given below:

$$\bar{H}_{cm} = -M [\bar{C}_{cm} \times \dot{\bar{C}}_{cm}] ;$$

$$\bar{H}_h = \sum_{i=1}^N \left[ \int_{m_i} (\bar{d}_i \times \dot{\bar{d}}_i) dm_i + \sum_{j=1}^{n_i} \int_{m_{i,j}} (\bar{d}_i + C_i^c \bar{d}_{ij}) \times (\dot{\bar{d}}_i + C_i^c \dot{\bar{d}}_{ij}) dm_{i,j} \right] ;$$

$$\begin{aligned} \bar{H}_{jr} = & \sum_{i=1}^N \left[ \int_{m_i} C_i^c (\bar{\rho}_i + \bar{\tau}_i + \bar{\delta}_i) \times \dot{C}_i^c (\bar{\rho}_i + \bar{\tau}_i + \bar{\delta}_i) dm_i \right. \\ & + \sum_{j=1}^{n_i} \int_{m_{i,j}} \{ C_i^c \bar{d}_{ij} + C_{i,j}^c \mu_{i,j} (\bar{\rho}_{ij} + \bar{\tau}_{ij} + \bar{\delta}_{ij}) \} \\ & \left. \times \{ \dot{C}_i^c \bar{d}_{ij} + (\dot{C}_{i,j}^c \mu_{i,j} + C_{i,j}^c \dot{\mu}_{i,j}) (\bar{\rho}_{ij} + \bar{\tau}_{ij} + \bar{\delta}_{ij}) \} dm_{i,j} \right] ; \end{aligned}$$

$$\begin{aligned} \bar{H}_t = & \int_{m_c} (\bar{\tau}_c \times \dot{\bar{\tau}}_c) dm_c + \sum_{i=1}^N \left[ \int_{m_i} (C_i^c \bar{\tau}_i \times (C_i^c \dot{\bar{\tau}}_i)) dm_i \right. \\ & \left. + \sum_{j=1}^{n_i} \int_{m_{i,j}} (C_{i,j}^c \mu_{i,j} \bar{\tau}_{ij}) \times (C_{i,j}^c \mu_{i,j} \dot{\bar{\tau}}_{ij}) dm_{i,j} \right] ; \end{aligned}$$

$$\begin{aligned} \bar{H}_v = & \int_{m_c} (\bar{\delta}_c \times \dot{\bar{\delta}}_c) dm_c + \sum_{i=1}^N \left[ \int_{m_i} (C_i^c \bar{\delta}_i \times (C_i^c \dot{\bar{\delta}}_i)) dm_i \right. \\ & \left. + \sum_{j=1}^{n_i} \int_{m_{i,j}} (C_{i,j}^c \mu_{i,j} \bar{\delta}_{ij}) \times (C_{i,j}^c \mu_{i,j} \dot{\bar{\delta}}_{ij}) dm_{i,j} \right] ; \end{aligned}$$

$$\begin{aligned}
 \bar{H}_{h,jr} &= \sum_{i=1}^N \left[ \int_{m_i} \bar{d}_i \times \dot{C}_i^c (\bar{\rho}_i + \bar{\tau}_i + \bar{\delta}_i) dm_i \right. \\
 &\quad \left. \sum_{j=1}^{n_i} \int_{m_{i,j}} \bar{d}_i \times \{ \dot{C}_{i,j}^c \bar{d}_{ij} + (C_{i,j}^c \mu_{i,j} + C_{i,j}^c \dot{\mu}_{i,j}) (\bar{\rho}_{ij} + \bar{\tau}_{ij} + \bar{\delta}_{ij}) \} dm_{i,j} \right]; \\
 \bar{H}_{h,r} &= \sum_{i=1}^N \left[ \int_{m_i} (C_i^c \bar{\rho}_i \times \dot{\bar{d}}_i) dm_i + \sum_{j=1}^{n_i} \int_{m_{i,j}} \{ C_{i,j}^c \mu_{i,j} \bar{\rho}_{ij} \times (\dot{\bar{d}}_i + C_i^c \dot{\bar{d}}_{ij}) \} dm_{i,j} \right]; \\
 \bar{H}_{h,t} &= \sum_{i=1}^N \left[ \int_{m_i} (C_i^c \bar{\tau}_i \times \dot{\bar{d}}_i + \bar{d}_i \times C_i^c \dot{\bar{\tau}}_i) dm_i \right. \\
 &\quad + \sum_{j=1}^{n_i} \int_{m_{i,j}} \{ C_{i,j}^c \mu_{i,j} \bar{\tau}_{ij} \times (\dot{\bar{d}}_i + C_i^c \dot{\bar{d}}_{ij}) \\
 &\quad \left. + (\bar{d}_i + C_i^c \bar{d}_{ij}) \times (C_{i,j}^c \mu_{i,j} \dot{\bar{\tau}}_{ij}) \} dm_{i,j} \right]; \\
 \bar{H}_{h,v} &= \sum_{i=1}^N \left[ \int_{m_i} (C_i^c \bar{\delta}_i \times \dot{\bar{d}}_i + \bar{d}_i \times C_i^c \dot{\bar{\delta}}_i) dm_i \right. \\
 &\quad + \sum_{j=1}^{n_i} \int_{m_{i,j}} \{ C_{i,j}^c \mu_{i,j} \bar{\delta}_{ij} \times (\dot{\bar{d}}_i + C_i^c \dot{\bar{d}}_{ij}) \\
 &\quad \left. + (\bar{d}_i + C_i^c \bar{d}_{ij}) \times (C_{i,j}^c \mu_{i,j} \dot{\bar{\delta}}_{ij}) \} dm_{i,j} \right]; \\
 \bar{H}_{\tau,t} &= \int_{m_c} (\bar{\rho}_c \times \dot{\bar{\tau}}_c) dm_c + \sum_{i=1}^N \left[ \int_{m_i} (C_i^c \bar{\rho}_i \times C_i^c \dot{\bar{\tau}}_i) dm_i \right.
 \end{aligned}$$

$$+ \sum_{j=1}^{n_i} \int_{m_{i,j}} (C_{i,j}^c \mu_{i,j} \bar{\rho}_{ij} \times C_{i,j}^c \mu_{i,j} \dot{\bar{\tau}}_{ij}) dm_{i,j} \Big];$$

$$\begin{aligned} \bar{H}_{r,v} = & \int_{m_c} (\bar{\rho}_c \times \dot{\bar{\delta}}_c) dm_c + \sum_{i=1}^N \left[ \int_{m_i} (C_i^c \bar{\rho}_i \times C_i^c \dot{\bar{\delta}}_i) dm_i \right. \\ & \left. + \sum_{j=1}^{n_i} \int_{m_{i,j}} (C_{i,j}^c \mu_{i,j} \bar{\rho}_{ij} \times C_{i,j}^c \mu_{i,j} \dot{\bar{\delta}}_{ij}) dm_{i,j} \right]; \end{aligned}$$

$$\begin{aligned} \bar{H}_{t,v} = & \int_{m_c} (\bar{\tau}_c \times \dot{\bar{\delta}}_c + \bar{\delta}_c \times \dot{\bar{\tau}}_c) dm_c + \sum_{i=1}^N \left[ \int_{m_i} (C_i^c \bar{\tau}_i \times C_i^c \dot{\bar{\delta}}_i + C_i^c \bar{\delta}_i \times C_i^c \dot{\bar{\tau}}_i) dm_i \right. \\ & + \sum_{j=1}^{n_i} \int_{m_{i,j}} \{ C_{i,j}^c \mu_{i,j} \bar{\tau}_{ij} \times (C_{i,j}^c \mu_{i,j} \dot{\bar{\delta}}_{ij}) \\ & \left. + C_{i,j}^c \mu_{i,j} \bar{\delta}_{ij} \times (C_{i,j}^c \mu_{i,j} \dot{\bar{\tau}}_{ij}) \} dm_{i,j} \right]. \end{aligned}$$

## Appendix B

### INPUT FILES FOR THE CMM

Input Data File for the Model:

```
* MSS data based on Julius's two arms model as of June 20, 1990
* Read in Ni, Nj
*
1 1 {Ni
*
* Modeb -- Modes for beam; Modepx -- Modes for plate in X
* Modepy -- Modes for plate in Y
1 1 1 {Modeb, Modepx, Modepy
*
* Nqc - central body g.c.
*
0 {Nqc
133.4d0 15.38d0 .0001d0 .00d0 .0d0 .3d0 {Rmi, RLi, WLi, TLi
2629.59d0 .0030d00 1.d0 0.0d0 .00d0 .00d0 {RIoi, RLi
-.5d0 -.5d0 0.0d0 {Ai
*
* Nqi(1) - 1st body g.c.
*
2 {Nqi
1.d0 1.d0 .0001d0 .10d0 .453562d2 .3d0 {Rmc, RLc, WLc, TLc
.3333d0 .7511d-3 1.d0 0.0d0 .00d0 .00d0 {RIoc, RLc
0.d0 0.0d0 .0d0 {Bi=.5 or .0665
0.d0 0.0d0 .5d0 {Ac
*
* Nqj(1) - 1st j body g.c.
*
1 2 {Nqj
1.d0 1.d0 .0001d0 .10d0 .453562d2 .3d0 {Rmi, RLi, WLi, TLi
.3333d0 .7511d-3 1.d0 0.0d0 .00d0 .00d0 {RIoi, RLi
1.0d0 .0d0 .0d0 {Bi
.0d0 .0d0 +.5d0 {Ai
```

Input Data File for the Mode:

```

* MAIN19D
*
  This is MSS model case
* long -longitude; inc - inclination;
* argu - argument; Ecc - eccentricity
1.570796  0.d0 1.570796  0.d0
* TOL - tolerance; HE - initial step size
*
  1.d-6  1.d-6
* METH - method; MITER -
* INDEX -
  1  0  1
* Nor - No. of Orbit; Npto - No. of points/Orbit
* Nstop - Termination of output; Nout -- Termination of vib. output
  1  1800  450  450
* Ncm - shift in cm; Nshade - Thermal Effect; Nengy - Evaluate energy
* Nang - use of alt. w; Nslew - Axis of slew
  1  0  0  1  3
* Shadei - Shadow angle; Tslew - Period of slew
* Aslew - angle of slew
  110.d0  36.d0 -180.d0
* Ncon -- nonlinear control
*
  0
* (Gp(i), Gv(i)) i=1 to 3
*
  0.64  1.6  0.64  1.6  0.64  1.6
*
* Y(iq), iq=1 to 7
*
0.0000d0 0.0000d0 0.0000d0  0.d0  0.d0  0.d0  0.d0
*
* Y(Nq+iq), iq=1 to 7
*
0.000d0 0.000d0 0.0000d0  0.d0  0.d0  0.d0  0.d0

```

## Appendix C

### INPUT DATA FILES FOR THE SMM

Data File for the INPUT I:

```
/PREP7
/OUTPUT,t1a_out
/COM 27TH DECEMBER 1990
/TITLE, MODAL ANALYSIS OF SPACE STATION (FEL - FIRST ELEMENT LAUNCH)

KAN,2
KAY,2,40
KAY,3
/COM DEFINE ELEMENT TYPES, 63=PLATE ELEMENT
/COM          4=BEAM ELEMENT
/COM          21=GENERALIZED MASS
ET,1,4
ET,2,21
/COM #####
/COM DEFINE MATERIAL PROPERTIES FOR CENTRAL TRUSS(BEAM)
EX,1,1.5E9
NUXY,1,0.333
R,1,3.464,1,1,1.86,1.86
DENS,1,45
/COM DEFINE MATERIAL PROPERTIES FOR MANIPULATOR (BEAM)
EX,2,1.E7
NUXY,2,0.333
R,2,3.464,1,1,1.86,1.86
DENS,2,61.66
/COM DEFINE MASS PROPERTIES FOR MSS PAYLOAD
R,3,1000,1000,1000,1,1,1
```

```
/COM #####  
/COM DEFINE NODES FOR MAIN TRUSS  
N,1,0.,57.5,0.  
N,21,0.,-57.5,0.  
FILL  
/COM DEFINE NODES FOR MANIPULATOR  
N,22,-0.1307,56.0,0.  
N,31,-1.307,42.56,0.  
FILL  
/COM  
NLIST,ALL  
/COM #####
```

```
/COM DEFINE ELEMENTS FOR MAIN TRUSS
```

```
TYPE,1  
REAL,1  
MAT,1
```

```
E,1,2  
E,2,3  
E,3,4  
E,4,5  
E,5,6  
E,6,7  
E,7,8  
E,8,9  
E,9,10  
E,10,11  
E,11,12  
E,12,13  
E,13,14  
E,14,15  
E,15,16  
E,16,17  
E,17,18  
E,18,19  
E,19,20  
E,20,21
```

/COM DEFINE ELEMENTS FOR MANIPULATOR

TYPE,1

MAT,2

REAL,2

E,1,22

E,22,23

E,23,24

E,24,25

E,25,26

E,26,27

E,27,28

E,28,29

E,29,30

E,30,31

/COM DEFINE ELEMENT FOR MANIPULATOR PAYLOAD

TYPE,2

REAL,3

E,31

/COM #####

WAVES

M,31,ALL

total,12

/SHOW,x11

/VIEW,1,1,1,1

ENUM

EPLLOT

ITER,1,1

AFWRITE

FINISH

/EXEC

/INPUT,27

FINISH



STRUCTURAL PROPERTIES FOR APPENDAGES

IMATXI => INERTIA MATRIX FOR APPENDAGES

APPENDAGE #1

1805.74D0 0.D0 0.D0
0.0D0 255000.00D0 0.D0
0.0D0 0.D0 255000.00d0

RHOIM => FIRST MOMENT OF AREA

Bc 0.D0 0.0D0 0.0D0
#1 39000.0D0 0.0D0 0.0D0

DI0 => INITIAL HINGE POSITION VECTOR FOR APPENDAGES

#1 0D0 0.D0 0.D0

EMASS => MASS PROPERTIES

Bc 17905.5D0
#1 4200.D0

ROTINI => 1-2-3 INITIAL RIGID ORIENTATION OF APPENDAGES

#1 0.D0 0.D0 0.D0

IMSL => IMSL: DGEAR PARAMETERS

HE => 1.D-8

TOL => 1.D-6

METH => 2

MITER => 0

INDEX => 1

SIMUL => SIMULATION RUN TIME

NOR => 0.20D0

NPTO => 10.d3

INICO => INITIAL CONDITIONS (IN DEGREES FOR ATTITUDE MOTION)

DISP0 => 0.D0 0.D0 0.d0 0.0D0 0.d0 0.d0 0.d0 0.d0 0.D0 0.D0 0.D0 0.D0 0.D0
VELO => 0.D0 0.D0

MODAL => MODAL EIGENVECTOR FILENAMES

-----  
STEP1 => MODAL EIGENVECTOR FILENAMES

-----  
mass0701  
mass0801  
mass0901  
mass1001  
mass1101

STEP2 => MODAL EIGENVECTOR FILENAMES

-----  
mass0702  
mass0802  
mass0902  
mass1002  
mass1102

.....

STEP35 => MODAL EIGENVECTOR FILENAMES

-----  
mass0735  
mass0835  
mass0935  
mass1035  
mass1135

STEP36 => MODAL EIGENVECTOR FILENAMES

-----  
mass0736  
mass0836  
mass0936  
mass1036  
mass1136

STEP37 => MODAL EIGENVECTOR FILENAMES

-----  
mass0737  
mass0837  
mass0937  
mass1037  
mass1137

%%%

OPTION => SIMULATION AND OUTPUT OPTIONS

-----  
ICTRL => 1 {0=UNCONTROLLED, 1=CONTROLLED }

IQUASI => 1 {1=OPEN LOOP , 2=CLOSE LOOP }

IGFOPT => 0 {1=INCLUDE G.F, 0= NO G.F. }

ISOLAR => 1 {0=DON'T PRINT, 1= PRINT }

IPVRAD => 0 {0=DON'T PRINT, 1= PRINT }

IRCS => 0 {0=DON'T PRINT, 1= PRINT }

ISTING => 0 {0=PRINT , 1= PRINT }

ITRUSSE => 1 {0=DON'T PRINT, 1= PRINT }

IAERO => 0 {1=INCLUDE AERO, 0= DO NOT }

IUPDAT => 1

-----  
EOF